(12) INTERNATIONAL APPLICATION PUBLISHED UNDER THE PATENT COOPERATION TREATY (PCT)

(19) World Intellectual Property Organization
International Bureau

(43) International Publication Date
12 October 2023 (12.10.2023)

WIPO | PCT

(10) International Publication Number
WO 2023/194339 A1

(51) International Patent Classification:
C07D 417/12 (2006.01) *A61P 3/00* (2006.01)

(21) International Application Number:
PCT/EP2023/058743

(22) International Filing Date:
04 April 2023 (04.04.2023)

(25) Filing Language: English

(26) Publication Language: English

(30) Priority Data:
22305456.0 05 April 2022 (05.04.2022) EP

(71) Applicant: **INVENTIVA** [FR/FR]; 50 rue de Dijon, 21121 DAIX (FR).

(72) Inventors: **BELL, Frédéric**; 7 ruelle des écoliers, 21380 MESSIGNY-ET-VANTOUX (FR). **BOUBIA, Benaissa**; 5 rue aux grands journaux, 21850 SAINT APOLLINAIRE (FR).

(74) Agent: **CABINET BEAU DE LOMENIE**; 158 Rue de l'Université, 75340 PARIS CEDEX 07 (FR).

(81) Designated States *(unless otherwise indicated, for every kind of national protection available)*: AE, AG, AL, AM, AO, AT, AU, AZ, BA, BB, BG, BH, BN, BR, BW, BY, BZ, CA, CH, CL, CN, CO, CR, CU, CV, CZ, DE, DJ, DK, DM, DO, DZ, EC, EE, EG, ES, FI, GB, GD, GE, GH, GM, GT, HN, HR, HU, ID, IL, IN, IQ, IR, IS, IT, JM, JO, JP, KE, KG, KH, KN, KP, KR, KW, KZ, LA, LC, LK, LR, LS, LU, LY, MA, MD, MG, MK, MN, MU, MW, MX, MY, MZ, NA, NG, NI, NO, NZ, OM, PA, PE, PG, PH, PL, PT, QA, RO, RS, RU, RW, SA, SC, SD, SE, SG, SK, SL, ST, SV, SY, TH, TJ, TM, TN, TR, TT, TZ, UA, UG, US, UZ, VC, VN, WS, ZA, ZM, ZW.

(84) Designated States *(unless otherwise indicated, for every kind of regional protection available)*: ARIPO (BW, CV, GH, GM, KE, LR, LS, MW, MZ, NA, RW, SC, SD, SL, ST, SZ, TZ, UG, ZM, ZW), Eurasian (AM, AZ, BY, KG, KZ, RU, TJ, TM), European (AL, AT, BE, BG, CH, CY, CZ, DE, DK, EE, ES, FI, FR, GB, GR, HR, HU, IE, IS, IT, LT, LU, LV, MC, ME, MK, MT, NL, NO, PL, PT, RO, RS, SE, SI, SK, SM, TR), OAPI (BF, BJ, CF, CG, CI, CM, GA, GN, GQ, GW, KM, ML, MR, NE, SN, TD, TG).

Published:
— *with international search report (Art. 21(3))*

(54) Title: CRYSTALLINE FORM OF LANIFIBRANOR

Fig.1

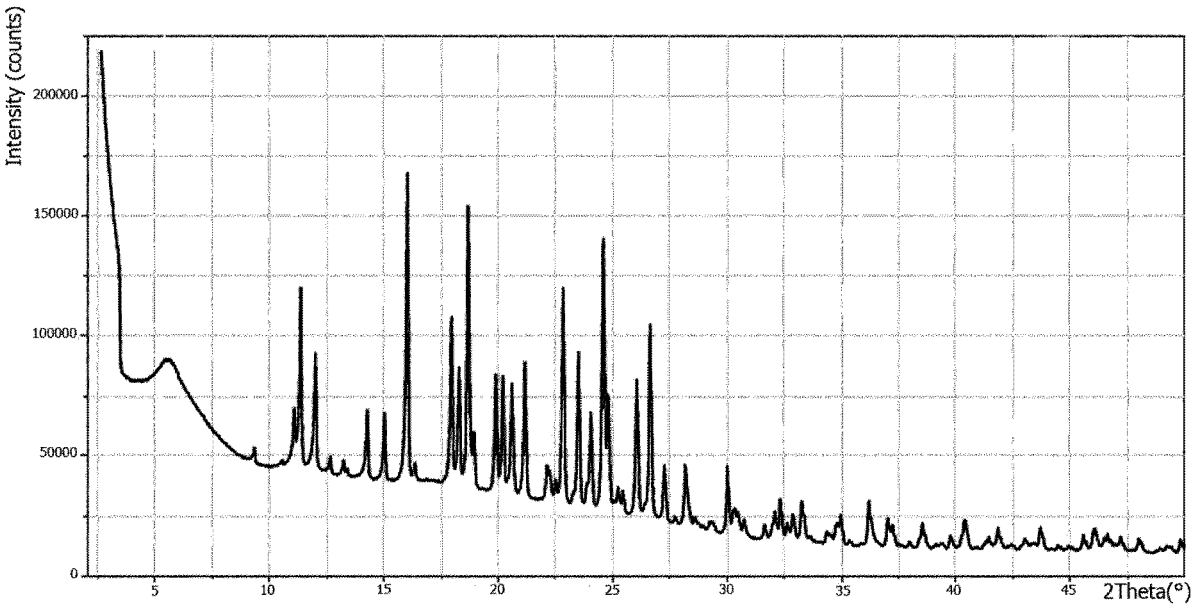

(57) Abstract: The present invention relates to a crystalline form of lanifibranor having an X-ray diffraction pattern in accordance with figure 1.

WO 2023/194339 A1

CRYSTALLINE FORM OF LANIFIBRANOR

FIELD OF THE INVENTION

The present invention relates to a crystalline form of lanifibranor, to pharmaceutical compositions containing said crystalline form, and to the use of said crystalline form in therapy.

BACKGROUND OF THE INVENTION

Lanifibranor or 1-(6-benzothiazolylsulfonyl)-5-chloro-1H-indole-2-butanoic acid is a pan-PPAR agonist which is currently in clinical development for the treatment of patients with non-alcoholic steatohepatitis (NASH), for which there is currently no approved therapy.

Lanifibranor is described as the free base in example 117 of WO 2007/026097, where it is obtained as a pale yellow powder having a melting point of 74-80°C. Crystalline forms of lanifibranor are disclosed in WO 2022/122014, WO 2022/143479, WO 2022/258060, WO 2022/261410 and WO 2023/016319.

The present invention provides a crystalline form of lanifibranor having desirable properties, such as high crystallinity, high purity, low hygroscopicity, favourable mechanical properties, and/or favourable stability.

SUMMARY OF THE INVENTION

In one aspect, the invention provides a crystalline form of lanifibranor (form beta). Form beta of lanifibranor is characterized by one or more of the following methods: (1) powder X-ray diffraction (PXRD); (2) differential scanning calorimetry (DSC); (3) thermogravimetry (TGA); (4) dynamic vapor sorption (DVS); (5) infrared spectroscopy (IR).

In another aspect, the invention provides a method for preparing crystalline form beta of lanifibranor, the method comprising heating a solution of lanifibranor in acetic acid and slowly cooling the resulting solution to room temperature.

In another aspect, the invention provides a pharmaceutical composition comprising crystalline form beta of lanifibranor and a pharmaceutically acceptable carrier or excipient.

In another aspect the invention provides a method of treating non-alcoholic fatty liver disease, which comprises administering to a subject in need thereof an effective amount of crystalline form beta of lanifibranor.

In another aspect the invention provides a method of treating a cirrhotic subject at risk of progressing from compensated stage to decompensated stage, which comprises administering to the subject an effective amount of crystalline form beta of lanifibranor.

In another aspect the invention provides crystalline form beta of lanifibranor for use in a

method of treating non-alcoholic fatty liver disease.

In another aspect the invention provides crystalline form beta of lanifibranor for use in a method of treating a cirrhotic subject at risk of progressing from compensated stage to decompensated stage.

DESCRPTION OF THE FIGURES

Figure 1 shows the PXRD pattern of form beta of lanifibranor.

Figure 2 shows the DSC curve of form beta of lanifibranor.

Figure 3 shows the TGA curve of form beta of lanifibranor.

Figure 4 shows the DVS isotherm plot of form beta of lanifibranor.

Figures 5A and 5B shows the IR spectrum of form beta of lanifibranor and the indexation of the absorption bands for the IR analysis.

Figure 6 shows a comparison of PXRD patterns of amorphous form (bottom curve), form beta (middle curve), and form alpha (top curve) of lanifibranor.

Figure 7 shows the DSC curve of form alpha of lanifibranor.

Figure 8 shows a comparison of DSC curves of amorphous form (bottom curve), form beta (middle curve), and form alpha (top curve) of lanifibranor.

Figures 9-14 show the PXRD patterns of a suspension of a mixture of lanifibranor forms alpha and beta in various solvents: acetone (figure 9), ethanol (figure 10), ethyl acetate (figure 11), acetic acid (figure 12), methyl ethyl ketone (figure 13) and methyl isobutyl ketone (figure 14). In each figure, the top curve is the PXRD pattern of lanifibranor form alpha; the top/middle curve is the PXRD pattern of the suspension at T0; the middle/bottom curve is the PXRD pattern of the suspension at T0+24h; the bottom curve is the PXRD pattern of lanifibranor form beta.

Figure 15 shows the PXRD pattern of lanifibranor form alpha before (top curve) and after (bottom curve) compression.

Figures 16-17 show a superimposition of the PXRD pattern of the solid form CSI described in WO 2022/122014 (bottom curve) with the PXRD pattern of lanifibranor form beta as shown in figure 1 (top curve).

Figures 18-19 show a superimposition of the PXRD pattern of the solid form CSII described in WO 2022/122014 (bottom curve) with the PXRD pattern of lanifibranor form beta as shown in figure 1 (top curve).

Figure 20 shows a superimposition of the PXRD pattern of the solid form CSIV described in WO 2022/122014 (bottom curve) with the PXRD pattern of lanifibranor form beta as shown in figure 1 (top curve).

Figure 21 shows a superimposition of the PXRD patterns of the solid forms described in WO 2022/143479 with the PXRD pattern of lanifibranor form beta as shown in figure 1. The following forms are represented, from top to bottom: lanifibranor form beta; lanifibranor cinnamamide co-crystal; lanifibranor p-toluenesulfonic acid co-crystal; lanifibranor tromethamine salt; lanifibranor form A.

Figure 22 shows a superimposition of the PXRD pattern of form A described in WO 2022/143479 (bottom curve) with the PXRD pattern of lanifibranor form alpha as shown in figure 1 (top curve).

Figure 23 shows a superimposition of the PXRD patterns of solid forms CM-A, CM-B and CM-F described in WO 2022/258060 with the PXRD pattern of lanifibranor form beta as shown in figure 1. The following forms are represented, from top to bottom: lanifibranor form beta; form CM-A; form CM-B; form CM-F.

Figure 24 shows a superimposition of the PXRD patterns of solid forms CM-C, CM-D, CM-E, CM-G and CM-I described in WO 2022/258060 with the PXRD pattern of lanifibranor form beta as shown in figure 1. The following forms are represented, from top to bottom: lanifibranor form beta; form CM-C; form CM-D; form CM-E; form CM-G; form CM-I.

Figure 25 shows a superimposition of the PXRD patterns of solid forms LN-1, LN-2, LN-3 and LN-4 described in WO 2022/261410 with the PXRD pattern of lanifibranor form beta as shown in figure 1. The following forms are represented, from top to bottom: lanifibranor form beta; form LN-1; form LN-2; form LN-3; form LN-4.

Figure 26 shows a superimposition of the PXRD pattern of form LN-1 described in WO 2022/261410 (bottom curve) with the PXRD pattern of lanifibranor form alpha as shown in figure 1 (top curve).

Figure 27 shows a superimposition of the PXRD patterns of solid forms CSV (embodiments 2 and 3) and CSIII described in WO 2023/016319 with the PXRD pattern of lanifibranor form beta as shown in figure 1. The following forms are represented, from top to bottom: lanifibranor form beta; form CSV (embodiment 2); form CSV (embodiment 3); form CSIII.

In all figures showing a PXRD pattern, the abscissa represents 2Theta (°) and the ordinate represents intensity (counts).

DETAILED DESCRIPTION OF THE INVENTION

As used herein, the term "lanifibranor" is understood to mean lanifibranor free acid, i.e. the compound of formula:

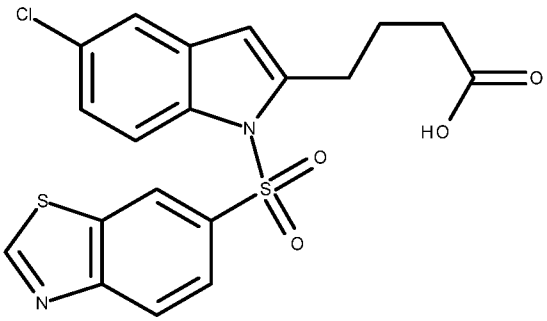

.

In one aspect, the invention provides a crystalline form of lanifibranor (form beta).

As described herein, lanifibranor (form beta) was characterized by one or more of the following methods: (1) powder X-ray diffraction (PXRD); (2) differential scanning calorimetry (DSC); (3) thermogravimetry (TGA). Such crystalline form may be further characterized by additional techniques, such as: (4) dynamic vapor sorption (DVS); and (5) infrared spectroscopy (IR).

In some embodiments of each aspect of the invention, form beta of lanifibranor is characterized by its PXRD pattern. One skilled in the art will appreciate that, with respect to X-ray diffraction peak positions (2θ), said positions will show some variability, typically as much as ±0.2°, such as for example ±0.1°. Further, one skilled in the art will appreciate that relative peak intensities will show inter-apparatus variability, as well as variability due to the degree of crystallinity, and should be taken as qualitative measures only.

In other embodiments of each aspects of the invention, lanifibranor (form beta) is characterized by its DSC curve. In still other embodiments of each aspects of the invention, lanifibranor (form beta) is characterized by its TGA curve.

It will be understood that various combinations of two, three or four techniques may be used to uniquely characterize lanifibranor (form beta) disclosed herein.

In one embodiment, lanifibranor (form beta) has a PXRD pattern comprising one, two, three, four, five or more than five peaks selected from the peaks in Table 1 (expressed in ° 2θ ± 0.2°).

In one embodiment, lanifibranor (form beta) has a PXRD pattern comprising one or more peaks at 2θ values selected from 16.0° ± 0.2°, 18.7° ± 0.2° and 24.6° ± 0.2° 2θ, as measured using an X-ray wavelength of 1.5406 Å. In some embodiments, form beta has a PXRD pattern further comprising at least one peak at 2θ values selected from 11.4° ± 0.2°, 18.0 ± 0.2°, 21.2 ± 0.2°, 22.8 ± 0.2°, 23.5 ± 0.2°, 26.1 ±0.2° and 26.7° ± 0.2° 2θ, as measured using an X-ray wavelength of 1.5406 Å.

In some of such embodiments, the PXRD pattern further comprises one or more additional

peaks at 2θ values selected from the peaks in Table 1.

Table 1

2θ position (°)	***Relative intensity***	***2θ position (°)***	***Relative intensity***
9.3	4.6%	28.2	20.5%
10.5	2.5%	28.6	3.3%
11.1	21.2%	28.7	1.7%
11.4	60.4%	29.0	1.0%
12.0	40.0%	29.2	3.0%
12.6	5.7%	29.4	3.1%
13.2	5.3%	30.0	23.2%
13.4	2.8%	30.3	9.6%
14.3	24.2%	30.5	8.1%
15.0	21.4%	30.7	5.5%
16.0	100.0%	31.7	4.5%
16.4	6.5%	32.1	8.9%
18.0	55.4%	32.3	13.6%
18.3	41.4%	32.7	5.5%
18.7	91.5%	32.9	9.1%
18.9	20.0%	33.2	14.0%
19.9	39.1%	33.3	9.9%
20.2	42.3%	33.6	1.8%
20.6	36.8%	34.4	4.3%
21.2	47.4%	34.5	3.4%
22.1	12.2%	34.8	8.0%
22.2	10.4%	35.0	9.6%
22.5	7.8%	35.4	1.5%
22.8	77.1%	36.2	14.6%
23.3	3.9%	36.3	11.2%
23.5	50.9%	36.5	1.5%
23.9	8.3%	37.0	10.0%
24.0	31.2%	37.2	7.3%
24.6	91.7%	38.0	1.7%
24.8	39.5%	38.1	1.0%
25.1	3.8%	38.4	3.9%
25.2	7.8%	38.5	8.7%
25.5	7.9%	38.6	5.2%
26.1	46.6%	39.1	1.5%
26.7	64.6%	39.4	1.8%
27.3	18.8%	39.8	4.3%
27.7	2.2%		

In one embodiment, the PXRD pattern of lanifibranor (beta form) is substantially in accordance with figure 1.

In one embodiment, lanifibranor (form beta) has a DSC curve comprising an endothermic peak at 182.3°C.

In one embodiment, the DSC curve of lanifibranor (form beta) is substantially in accordance with figure 2.

In one embodiment, the TGA curve of lanifibranor (form beta) does not highlight any significant weight loss over the temperature range 25 - 200°C. Above 250°C, the weight loss observed likely corresponds to degradation.

In one embodiment, the TGA curve of lanifibranor (form beta) is substantially in accordance with figure 3.

In one embodiment, the DVS analysis performed on lanifibranor (form beta) does not exhibit significant weight variations over the range of relative humidity values investigated: a maximum uptake of + 0.1% was observed on the range 0% RH – 95% RH .

In one embodiment, the DVS isotherm plot of lanifibranor (form beta) is substantially in accordance with figure 4.

In one embodiment, the IR spectrum of lanifibranor (form beta) is substantially in accordance with figure 5.

In another aspect, the invention provides a method for preparing lanifibranor (form beta), the method comprising a) heating a solution of lanifibranor in acetic acid, at a temperature in the range of about 100°C to about 110°C, and b) cooling the resulting solution to room temperature.

In one embodiment, step a) is performed at a temperature of about 105°C.

In one embodiment, step a) and step b), as defined above, are repeated at least once. For example the method for preparing lanifibranor (form beta) may comprise the steps of:

- heating a solution of lanifibranor in acetic acid, at a temperature in the range of about 100°C to about 110°C,
- allowing the solution to return to room temperature,
- heating a solution of product (as recovered from the cooled solution) in acetic acid, at a temperature in the range of about 100°C to about 110°C,
- cooling the solution to room temperature.

Lanifibranor free acid can be obtained e.g. as described in WO 2007/026097 or as described in example 1 below.

When screening for solid forms of lanifibranor, the inventors identified two crystalline forms of the compound, one form being unstable in the sense that it did readily convert to the other form upon handling/processing. The unstable form was labelled "form alpha" and the more stable form was labelled "form beta". An amorphous form was further obtained. The amorphous form was found to crystallize into form alpha or form beta even at low

temperatures. It was further found that the process for preparing form beta, where acetic acid is used for crystallization, makes it possible to scale up the manufacture of this crystalline form, to obtain batches of up to about 150 kg.

Lanifibranor form beta can be used as the active ingredient of a pharmaceutical composition. Thus, in another aspect, the invention provides a pharmaceutical composition comprising lanifibranor (form beta) and a pharmaceutically acceptable carrier or excipient. The expression "pharmaceutically acceptable carrier or excipient" means that the excipient or carrier is suitable for incorporation into a pharmaceutical composition and is compatible with the other ingredients of the composition. Particularly, it is not toxic. Its use allows facilitating the preparation, preservation and administration of the active ingredient. Such excipients and carriers are well-known to the person skilled in the art, and are described in the French and/or European Pharmacopoeia. Examples of pharmaceutical carriers include, but not limited to, any suitable solvents, dispersion media, coatings, antibacterial and antifungal agents and isotonic agents, and examples of excipients that may also be components of the formulation include fillers, binders, disintegrating agents and lubricants.

In another aspect the invention provides a method of treating non-alcoholic fatty liver disease (NAFLD), which comprises administering to a subject in need thereof an effective amount of lanifibranor (form beta).

In one embodiment, NAFLD includes non-alcoholic fatty liver (NAFL) and non-alcoholic steatohepatitis (NASH).

In another aspect the invention provides a method of treating a cirrhotic subject at risk of progressing from compensated stage to decompensated stage, which comprises administering to the subject an effective amount of lanifibranor (form beta).

In another aspect the invention provides lanifibranor form beta for use in a method of treating non-alcoholic fatty liver disease.

In another aspect the invention provides lanifibranor form beta for use in a method of treating a cirrhotic subject at risk of progressing from compensated stage to decompensated stage.

In another aspect the invention provides for the use of lanifibranor form beta as defined above for the preparation of a medicament intended for the treatment of non-alcoholic fatty liver disease (NAFLD). In some embodiments, NAFLD includes non-alcoholic fatty liver and non-alcoholic steatohepatitis.

In another aspect the invention provides for the use of lanifibranor form beta as defined above for the preparation of a medicament intended for the treatment of cirrhosis in

compensated stage, especially for preventing the decompensation of cirrhosis.

The invention is illustrated by the examples below.

EXAMPLES

Abbreviations

MeTHF = 2-methyl tetrahydrofuran

MTBE = methyl *tert*-butyl ether

NAC = N-acetyl-L-cysteine

$PdCl_2(PPh_3)_2$ = bis(triphenylphosphine)palladium(II) dichloride

THF = tetrahydrofuran

PXRD

Powder X-ray diffraction analysis was conducted using a Panalytical Empyrean S3 diffractometer equipped with a Cu radiation source (Cu wavelength = 1.5406 Å). Analyses were performed in transmission mode (samples were placed between Kapton® and polypropylene foils), on the angular range 2θ = 2 - 50 °, with a step size of 0.026 ° and a time per step of 20.4 s.

DSC

DSC analysis was conducted on a Mettler Toledo DSC3+ calorimeter. Analyses were performed on a few milligrams of sample, in 40 µL sealed aluminum pans, punctured before analysis, under nitrogen flush at 50 mL/min. A temperature range between 20°C and 300°C was scanned at a 10°C/min rate.

TGA

TGA analysis was conducted on a Mettler Toledo TGA/DSC3+ thermogravimetric analyzer. Analyses were performed on a few milligrams of sample, in 100 µL sealed aluminum pans, punctured before analysis, under nitrogen flush at 50 mL/min. A temperature range between 25°C and 300°C was scanned at a 10°C/min rate.

DVS

DVS analysis was conducted on a SMS DVS Intrinsic system. Analyses were performed on a few milligrams of sample, in open aluminum pans at 25°C. The stability criterion for each step was a weight change lower than 0.002% on a 5 min time frame. The time criterion for each step was 100 min (minimum duration by step: 10 min). Relative humidity was scanned between 0% RH and 95% RH with 10% RH steps (40 – 0 – 95 – 0 – 95).

IR

IR analysis was conducted on a Nicolet™ iS5 spectrometer equipped with an ATR iD7 accessory. Analyses were performed in ATR mode from 4000 cm^{-1} to 525 cm^{-1} (resolution of

4 cm^{-1}), with 32 scans for background and measurement.

Example 1: lanifibranor free acid

Degassed triethylamine (200 mL) was added to a solution of N-(4-chloro-2-iodo-phenyl)-1,3-benzothiazole-6-sulfonamide in THF, followed by the addition of $PdCl_2(PPh_3)_2$ (1.17 g), CuI (0.85 g) and 5-hexynoic acid (CAS [53293-00-8]) (14.3 g). The reaction mixture was stirred at 40 °C for 3 hours. The mixture was concentrated under reduced pressure at 40 °C until 5 volumes of solution remained relative to the weight of the sulphonamide starting material. Water (3 volumes) was added, and the residual THF was removed by distillation. The mixture was washed with MTBE (2 volumes) 3 times. The aqueous phase was treated with a mixture of MeTHF and HCl (37%). The MeTHF solution was washed with a 6% aqueous solution of NAC (twice). The washing was performed by stirring the organic phase with 20% w/w of NAC at 60°C for 1 hour. The organic phase was then washed twice and the NAC phases were combined and washed with pure water (three times). As previously, the washing was performed by stirring the NAC phase with water at 60°C for 1 hour. The MeTHF solution was heated at 60°C. Shirasagi A Charcoal (0.5%) was added (w/w relative to the quantity of starting sulfonamide) and the suspension was stirred at 60°C for 30 minutes. The mixture was then filtered on a dicalite bed and washed abundantly with MeTHF. The lanifibranor-containing solution obtained was used as such in the next example.

Example 2: lanifibranor (form beta)

The solution obtained in example 1 was concentrated. Acetic acid was added to the residue and the solution was concentrated. The suspension was heated at 105°C, and acetic acid was added in small portions until complete dissolution. The solution was then stirred at 105°C for 1 hour, and left to slowly cool down to room temperature under stirring. The solid product obtained was filtered on a sintered glass G4 filter and washed twice with acetic acid to give 41.63 g of product (86.3% yield) with a HPLC purity of 99.8%. 41.3 g of product were suspended in acetic acid and the suspension was stirred at 105°C for 1 hour. After complete dissolution, the mixture was left to cool down to room temperature in stages, filtered on a sintered glass G4 filter, and washed with acetic acid. The product collected was dried under vacuum at 60°C for 5 hours to afford 38.6 g (93.5% yield) of the title compound.

APCI MS m/z 435 [M+H]+; UPLC-MS (210-260 nm) purity: 99.9%.

^{1}H NMR (500 MHz DMSO-d6): δ 1.86-2.01 (2H, quint, J= 7.5 Hz); 2.36 (2H, t, J=7.5 Hz); 3.09 (2H, t, J=7.5 Hz); 6.62 (1H, s); 7.32 (1H, dd, J= 2.0 Hz et J= 8.5 Hz); 7.57 (1H, d, J=2.5 Hz); 7.85 (1H, dd, J=2.0 et J=8.5 Hz); 8.09 (1H, d, J=8.5 Hz); 8.20 (1H, d, J=8.5 Hz);

8.97 (1H, d, J=2.0 Hz); 9.67 (1H, s); 12.14 (1H, s).

Form beta of lanifibranor was characterized by PXRD (figure 1), DSC (figure 2), TGA (figure 3), DVS (figure 4) and IR (figures 5A and 5B). It can be seen from figure 2 that lanifibranor (form beta) has a DSC curve comprising an endothermic peak at 182.3°C.

Example 3: lanifibranor (form alpha)

A homogenous solution was prepared by dissolving form beta of lanifibranor (10g), as obtained in example 2, in acetic acid (7.5 volumes) at 98°C. The solution was then quenched by stirring the mixture at 5°C under precipitation occurred. The temperature of the mixture was monitored and, once it reached 20°C, the solid phase was recovered by filtration on n°3 sintered glass filter. The solid recovered was dried at 60°C under vacuum and kept at room temperature.

Form alpha of lanifibranor was characterized by PXRD (Table 2 and figure 6) and DSC (figure 7). It can be seen from figure 7 that form alpha has a DSC curve comprising an endothermic peak at 180.8°C.

Table 2

2θ position (°)	***Relative intensity***	***2θ position (°)***	***Relative intensity***
7.8	79.6%	27.5	8.1%
8.4	4.7%	27.7	8.1%
10.9	37.7%	28.2	18.8%
11.9	1.9%	28.9	7.6%
12.5	5.9%	29.2	6.9%
12.7	7.1%	29.5	1.4%
13.7	5.8%	29.8	11.5%
14.0	27.1%	30.0	4.1%
15.6	28.3%	30.2	2.2%
16.5	71.0%	30.5	9.1%
16.8	10.9%	30.8	3.9%
17.0	52.8%	31.1	1.9%
17.6	5.9%	31.9	4.1%
17.9	53.0%	32.3	5.5%
19.2	44.9%	32.4	2.2%
19.9	9.8%	33.1	8.6%
20.2	89.6%	33.3	8.6%
20.4	4.7%	33.8	2.5%
21.2	39.4%	33.9	3.4%
21.6	1.6%	34.1	2.8%
21.9	3.0%	34.5	1.3%
22.3	100.0%	34.9	2.5%
22.5	29.6%	35.0	4.2%
23.2	28.9%	35.7	3.4%
23.3	35.8%	35.9	8.4%
23.9	20.8%	36.3	12.6%

24.1	72.1%	36.5	2.3%
24.5	56.8%	37.2	1.1%
25.0	6.0%	37.4	1.7%
25.3	14.1%	38.1	2.3%
25.6	28.3%	38.2	4.1%
26.0	14.1%	38.4	2.2%
26.4	23.0%	38.5	1.5%
26.8	4.8%		

Example 4: lanifibranor (amorphous form)

A homogenous solution was prepared by dissolving 1 g of lanifibranor (form beta), as obtained in example 2, in 35 mL of acetone, at 50°C. The solution was then fully evaporated under vacuum at 50°C. The solid phase was then recovered, dried overnight under vacuum, at room temperature, and stored at -26°C.

The amorphous form of lanifibranor was characterized by PXRD (see figure 6).

Example 5: stability tests

Competitive slurry tests were performed in various solvents such as acetone, ethanol, ethyl acetate, acetic acid, methyl ethyl ketone and methyl isobutyl ketone.

A saturated solution of lanifibranor form beta (as obtained in example 2) was prepared for each solvent. An equal amount of lanifibranor form alpha and lanifibranor form beta was introduced into a vial (50 mg + 50 mg), and 250 µL of the saturated solution prepared beforehand (recovered by filtration through a 0.2 µm H-PTFE filter) were then added. The mixture was stirred at room temperature, samples of the solid were taken immediately after stirring was initiated and 24 hours after, and analyzed by PXRD to identify the solid form(s) present. The results are presented in Table 2.

Table 2

Solvent	**Form(s) present T0**	**Form(s) present T0 + 24h**
Acetone	form alpha + form beta	form beta
Ethanol	form alpha + form beta	form beta
Ethyl acetate	form alpha + form beta	form beta
Acetic acid	form alpha + form beta	form beta
Methyl ethyl ketone	form alpha + form beta	form beta
Methyl isobutyl ketone	form alpha + form beta	form beta

It can be seen that after 24 h a total conversion towards lanifibranor form beta is observed in all solvents considered. Form beta is therefore the most stable form at room temperature.

Example 7: compression tests

Compression tests were performed on the crystalline forms (alpha, beta) and on the amorphous form of lanifibranor.

100 mg of each sample were introduced between anvils into a 13 mm die and subjected to a 10-Ton pressure for 15 minutes. The pellet obtained was then de-compacted and analysed by PXRD in order to monitor changes in the crystal structure of the sample.

For lanifibranor form alpha (see figure 15), an enlargement of the diffraction peaks, a decrease of their intensities and additional signals that could correspond to peak shifts caused by a transformation to form beta were observed after compression. A signal characteristic of amorphous material was also highlighted.

For lanifibranor form beta (diffraction pattern not shown), a decrease of the crystallinity was observed after compression (peaks enlargement, decrease of intensity), but no significant change in the solid form was observed.

For the amorphous form (diffraction pattern not shown), weak diffraction signals corresponding to form beta were detected after compression, indicating the start of crystallization in the sample.

Example 8: comparison between lanifibranor form beta and lanifibranor as obtained in example 117 of WO 2007/026097

Lanifibranor was prepared following the procedure described in example 117 of WO 2007/026097. A white amorphous powder was obtained in about 75% yield, with a melting point (measured on a Kofler bench) in the range 74-76°C. The product obtained was found to be amorphous, with a PXRD pattern comparable to that shown in Figure 6.

Example 9: comparison between lanifibranor form beta and the solid forms disclosed in WO 2022/122014

The PXRD patterns of the solid forms described in WO 2022/122014, namely form CSI (examples 2 and 3), form CSII (examples 5 and 6), and form CSIV (example 7), were digitized and then compared (by superimposition) to the PXRD pattern of lanifibranor form beta (as shown in figure 1). The results are shown in figures 16-17 (CSI), 18-19 (CSII) and 20 (CSIV). It can be concluded from these figures that none of the PXRD patterns described in WO 2022/122014 match with the PXRD pattern of lanifibranor form beta.

Example 10: comparison between lanifibranor form beta and the solid forms disclosed in WO 2022/143479

The PXRD patterns of the solid forms described in WO 2022/143479, namely lanifibranor cinnamamide co-crystal (examples 1-6), lanifibranor p-toluenesulfonic acid co-crystal (examples 7-11), lanifibranor tromethamine salt (examples 12-16), and form A (examples 17-20), were digitized and then compared (by superimposition) to the PXRD pattern of lanifibranor form beta (as shown in figure 1). The results are shown in figure 21. It can be concluded from this figure that none of the PXRD patterns described in WO 2022/143479 match with the PXRD pattern of lanifibranor form beta. By contrast, and as shown in figure 22, the PXRD pattern of form A described in WO 2022/143479 substantially matches with the PXRD pattern of lanifibranor form alpha (as shown in figure 6).

Example 11: comparison between lanifibranor form beta and the solid forms disclosed in WO 2022/258060

The PXRD patterns of the solid forms described in WO 2022/258060, namely lanifibranor solid forms CM-A, CM-B, CM-C, CM-D, CM-E, CM-F, CM-G and CM-I, were digitized and then compared (by superimposition) to the PXRD pattern of lanifibranor form beta (as shown in figure 1). The results are shown in figure 23 (forms CM-A, CM-B and CM-F) and figure 24 (forms CM-C, CM-D, CM-E, CM-G and CM-I). It can be concluded from these figures that none of the PXRD patterns described in WO 2022/258060 match with the PXRD pattern of lanifibranor form beta. In addition, the PXRD patterns of the solid forms described in WO 2022/258060 do not match either with the PXRD pattern of lanifibranor form alpha (data not shown).

Example 12: comparison between lanifibranor form beta and the solid forms disclosed in WO 2022/261410

The PXRD patterns of the solid forms described in WO 2022/261410, namely lanifibranor forms LN-1, LN-2, LN-3 and LN-4, were digitized and then compared (by superimposition) to the PXRD pattern of lanifibranor form beta (as shown in figure 1). The results are shown in figure 25. It can be concluded from this figure that none of the PXRD patterns described in WO 2022/261410 match with the PXRD pattern of lanifibranor form beta. By contrast, and as shown in figure 26, the PXRD pattern of form LN-1 described in WO 2022/261410 substantially matches with the PXRD pattern of lanifibranor form alpha (as shown in figure 6).

Example 13: comparison between lanifibranor form beta and the solid forms disclosed in WO 2023/016319

The PXRD patterns of the solid forms described in WO 2023/016319, namely lanifibranor forms CSV (embodiments 2 and 3) and CSIII, were digitized and then compared (by superimposition) to the PXRD pattern of lanifibranor form beta (as shown in figure 1). The results are shown in figure 27. It can be concluded from this figure that none of the PXRD patterns described in WO 2023/016319 match with the PXRD pattern of lanifibranor form beta. In addition, the PXRD patterns of the solid forms described in WO 2023/016319 do not match either with the PXRD pattern of lanifibranor form alpha (data not shown).

Example 14: stability test

Lanifibranor form beta, as obtained in example 2, was submitted to stability testing in accordance with EMA guidance (CPMP/ICH/2736/99, last revised in August 2003); the drug substance was thus stored under the following conditions:

6 months at 30°C/65°RH,

6 months at 40°C/75%RH, and

12 months at 25°C/60%RH.

At the end of each storage period, the drug substance was characterized by PXRD and by DSC. In each case, the PXRD pattern was characteristic of lanifibranor form beta as shown in figure 1, and the DSC curve was characteristic of lanifibranor form beta (endothermic peak at 182.3°C), indicating that lanifibranor form beta is stable over long-term storage.

CLAIMS

1. A crystalline form of lanifibranor (form beta) having an X-ray powder diffraction pattern comprising peaks at 16.0° ± 0.2°, 18.7° ± 0.2° and 24.6° ± 0.2° 2θ, as measured using an X-ray wavelength of 1.5406 Å.

2. The crystalline form of claim 1, wherein the X-ray diffraction pattern further comprises at least one peak at 2θ values selected from: 11.4° ± 0.2°, 18.0 ± 0.2°, 21.2 ± 0.2°, 22.8 ± 0.2°, 23.5 ± 0.2°, 26.1 ±0.2° and 26.7° ± 0.2° 2θ, as measured using an X-ray wavelength of 1.5406 Å.

3. The crystalline form of one of claims 1 or 2, wherein the X-ray diffraction pattern is substantially in accordance with figure 1.

4. The crystalline form of one of claims 1 to 3, having a differential scanning calorimetry (DSC) curve comprising an endothermic peak at 182.3°C.

5. The crystalline form of claim 4, wherein the DSC curve is substantially in accordance with figure 2.

6. A process for preparing the crystalline form of any of claims 1 to 5, comprising:
a) heating a solution of lanifibranor in acetic acid, at a temperature in the range of about 100°C to about 110°C, and
b) cooling the resulting solution to room temperature.

7. The process of claim 6, wherein step a) is performed at a temperature of about 105°C.

8. The process of claim 6 or claim 7, wherein step b) is performed in stages.

9. A pharmaceutical composition comprising the crystalline form of any of claims 1 to 5 and a pharmaceutically acceptable carrier or excipient.

10. Lanifibranor form beta as defined in any of claims 1 to 5, for use in a method of

treating non-alcoholic fatty liver disease (NAFLD).

11. Lanifibranor form beta for use of claim 10, wherein NAFLD includes non-alcoholic fatty liver and non-alcoholic steatohepatitis.

12. Lanifibranor form beta as defined in any of claims 1 to 5, for use in a method of treating a cirrhotic subject at risk of progressing from compensated stage to decompensated stage.

13. A method of treating non-alcoholic fatty liver disease (NAFLD), which comprises administering to a subject in need thereof an effective amount of lanifibranor form beta as defined in any of claims 1 to 5.

14. The method of claim 13, wherein NAFLD includes non-alcoholic fatty liver and non-alcoholic steatohepatitis.

15. A method of treating a cirrhotic subject at risk of progressing from compensated stage to decompensated stage, which comprises administering to the subject an effective amount of lanifibranor form beta as defined in any of claims 1 to 5.

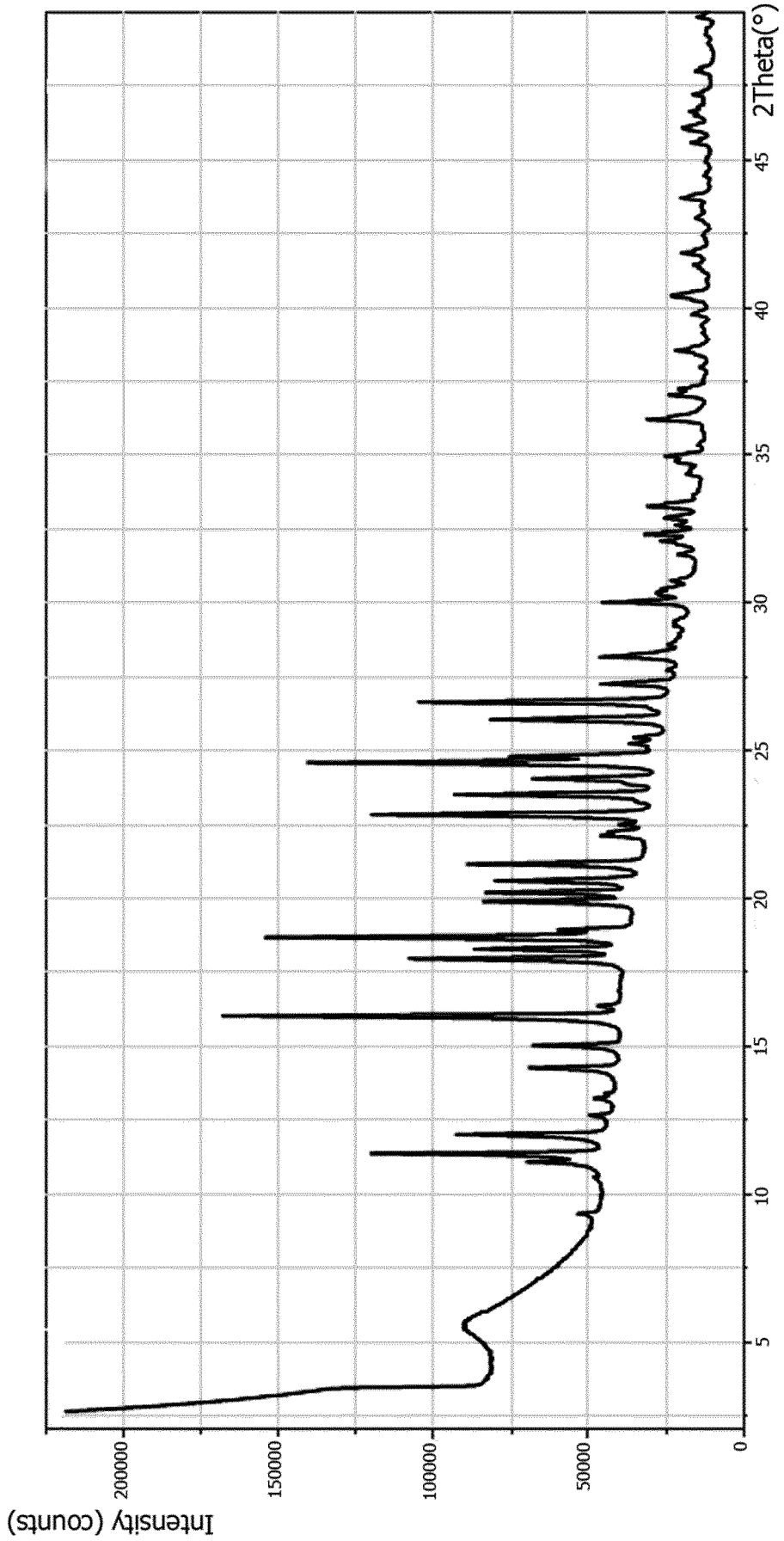
Intensity (counts)
200000
150000
100000
50000
0
5
10
15
20
25
30
35
40
45
2Theta(°)

Fig.1

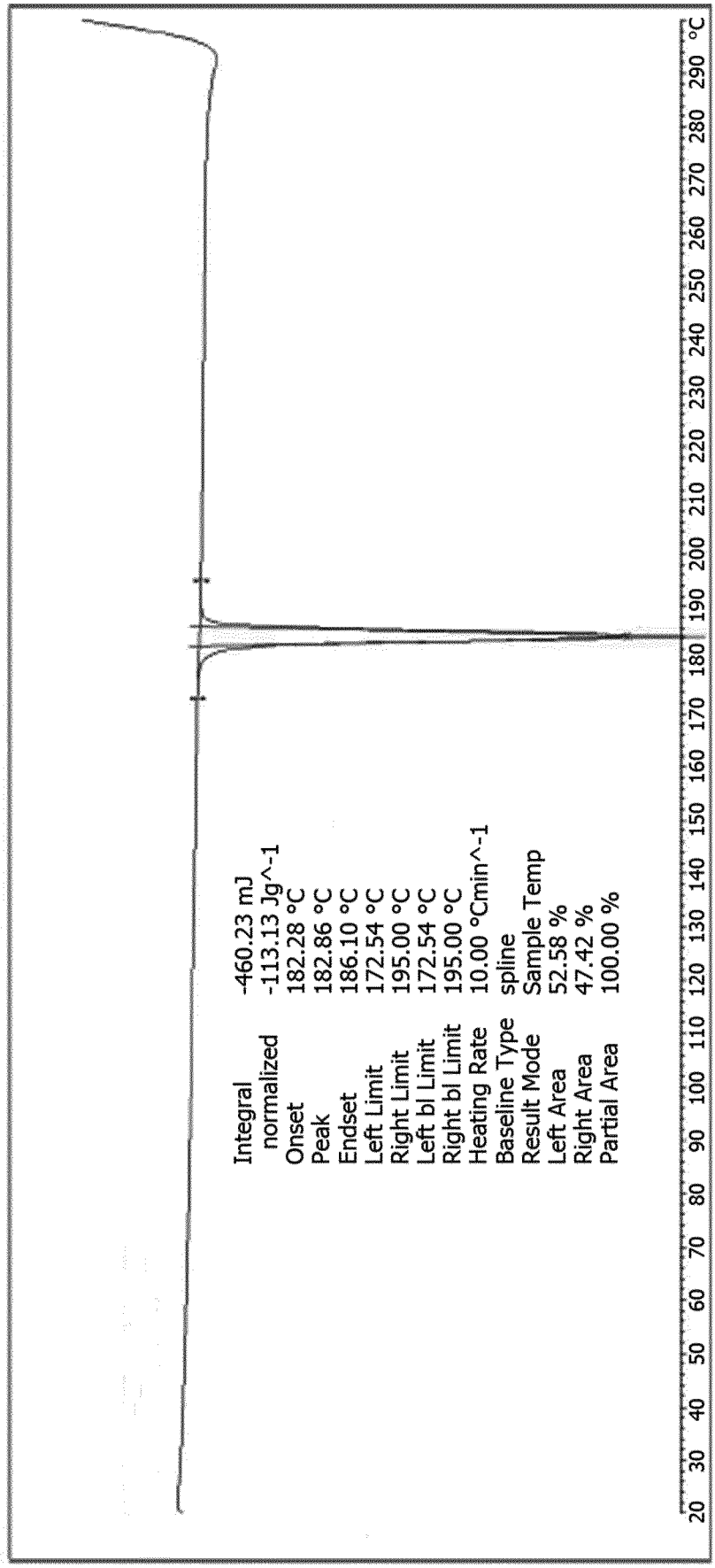
Integral -460.23 mJ
normalized -113.13 Jg^-1
Onset 182.28 °C
Peak 182.86 °C
Endset 186.10 °C
Left Limit 172.54 °C
Right Limit 195.00 °C
Left bl Limit 172.54 °C
Right bl Limit 195.00 °C
Heating Rate 10.00 °Cmin^-1
Baseline Type spline
Result Mode Sample Temp
Left Area 52.58 %
Right Area 47.42 %
Partial Area 100.00 %
20 30 40 50 60 70 80 90 100 110 120 130 140 150 160 170 180 190 200 210 220 230 240 250 260 270 280 290 °C

Fig.2

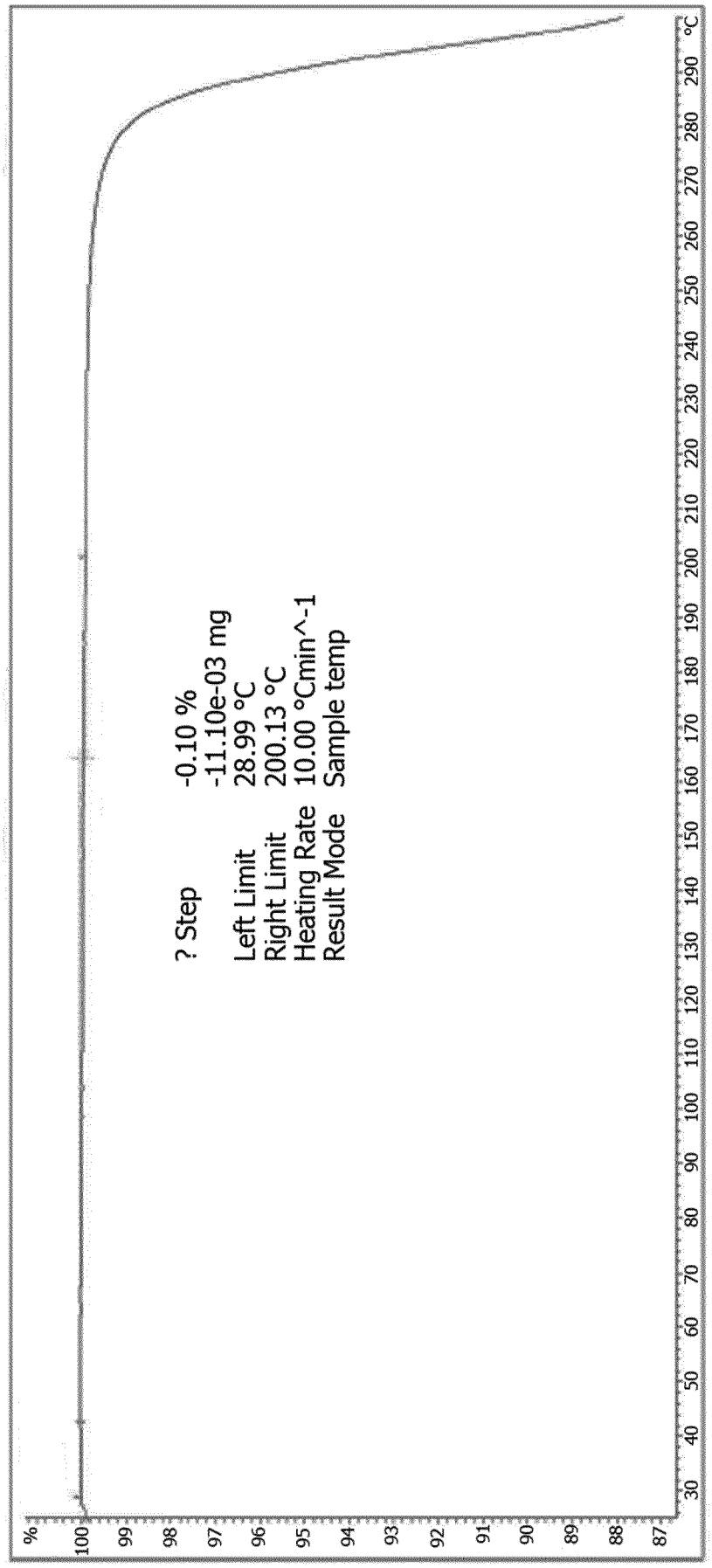
? Step -0.10 %
-11.10e-03 mg
Left Limit 28.99 °C
Right Limit 200.13 °C
Heating Rate 10.00 °Cmin^-1
Result Mode Sample temp
%
°C

Fig.3

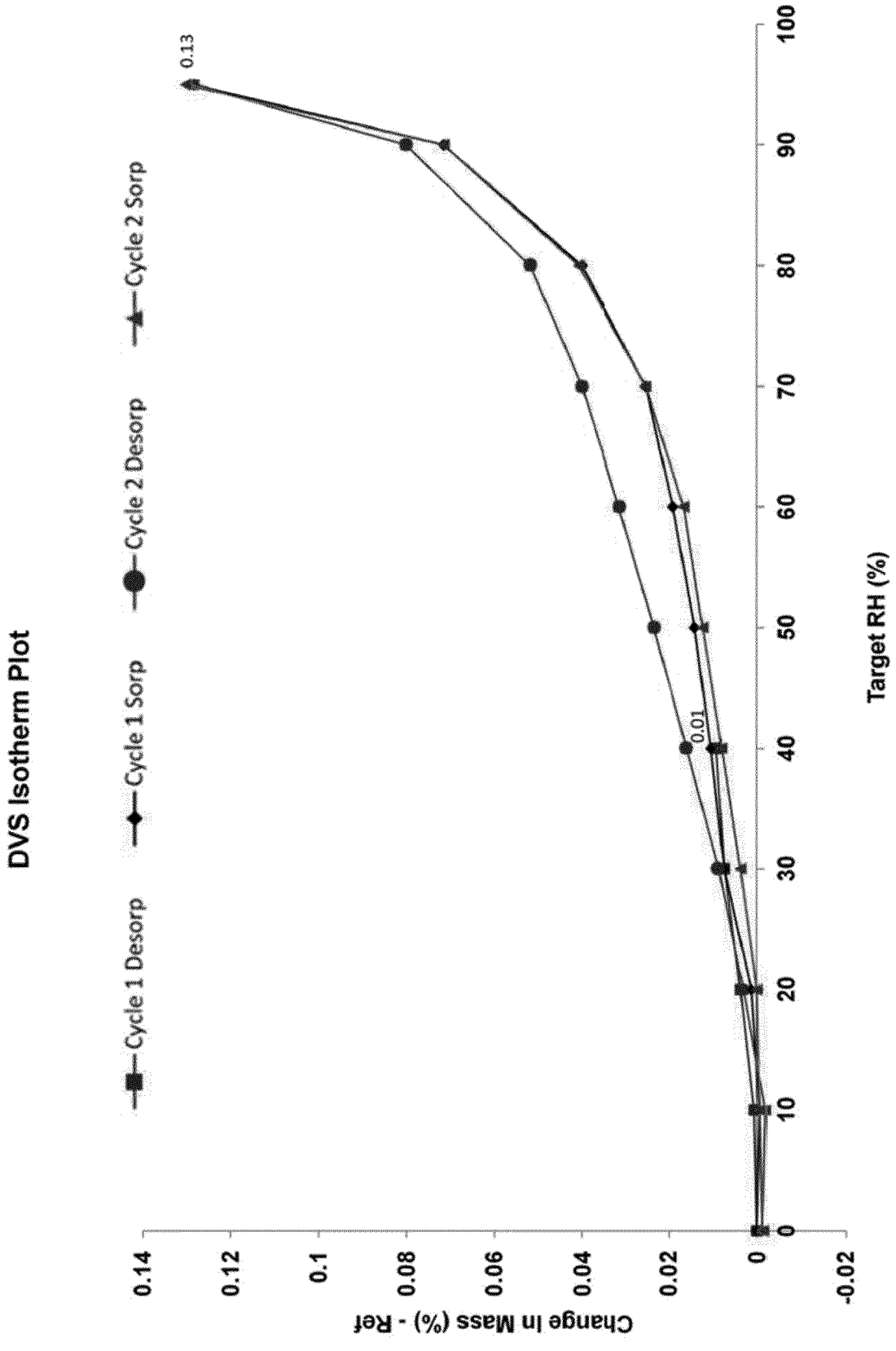
DVS Isotherm Plot
Cycle 1 Desorp
Cycle 1 Sorp
Cycle 2 Desorp
Cycle 2 Sorp
0.13
0.01
Change In Mass (%) - Ref
0.14
0.12
0.1
0.08
0.06
0.04
0.02
0
-0.02
Target RH (%)
0
10
20
30
40
50
60
70
80
90
100

Fig.4

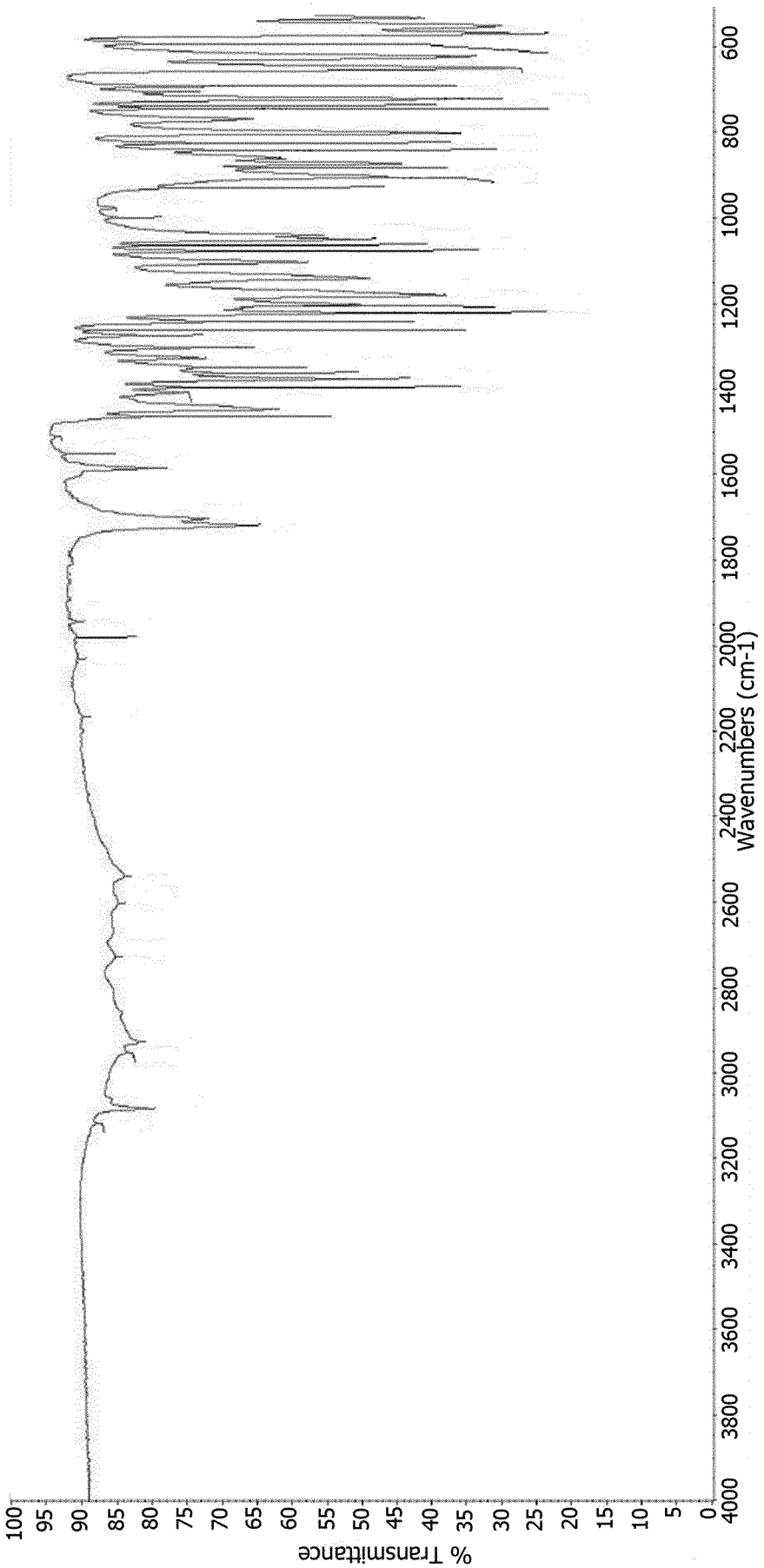
% Transmittance
100
95
90
85
80
75
70
65
60
55
50
45
40
35
30
25
20
15
10
5
0
4000
3800
3600
3400
3200
3000
2800
2600
2400
2200
2000
1800
1600
1400
1200
1000
800
600
Wavenumbers (cm-1)

Fig.5A

Position (cm-1)	Transmittance (%)	Position (cm-1)	Transmittance (%)	Position (cm-1)	Transmittance (%)
529.55	41.147	973.99	85.212	1393.16	75.569
548.63	30.456	996.63	84.796	1406.05	75.414
565.82	27.158	1038.11	55.947	1445	62.46
589.85	81.354	1047.15	51.589	1462.67	80.914
619.54	34.208	1062.33	81.823	1508.63	93.457
647.15	27.473	1075.51	73.452	1550.31	91.852
689.86	72.768	1101.69	58.493	1583.43	80.572
702.54	77.98	1138.71	49.411	1701.58	72.171
718.96	38.89	1177.7	37.876	1717.14	67.515
735.3	83.077	1200.22	50.453	1941.99	90.624
741.51	77.263	1208.69	66.768	1978.4	90.556
766.26	66.164	1219.86	53.711	2029.19	90.412
798.39	38.795	1240.39	72.444	2166.44	89.676
822.19	73.835	1260.75	88.704	2537.11	83.835
839.83	70.71	1272.63	81.826	2599.81	84.657
858.46	61.18	1301.78	74.393	2726.44	85.182
870.57	44.136	1325.23	73.2	2926.06	81.714
881	63.993	1347.72	73.881	2950.39	83.316
901.02	46.341	1360.34	70.733	3081.6	80.355
927.33	77.339	1374.07	52.166	3116.56	87.751
Threshold: 93.667; Sensitivity: 81					

Fig.5B

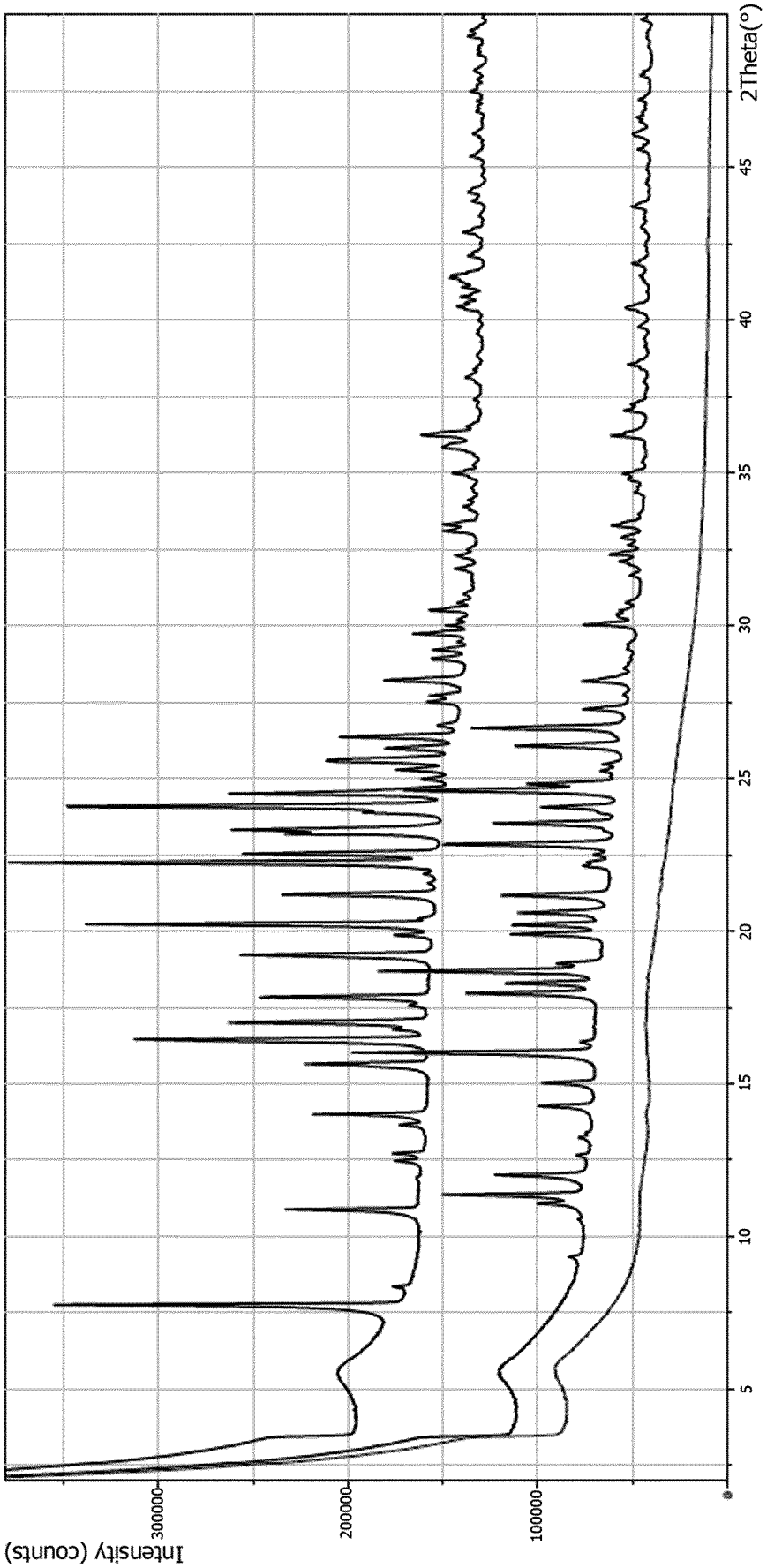
2Theta(°)
5
10
15
20
25
30
35
40
45
Intensity (counts)
100000
200000
300000

Fig.6

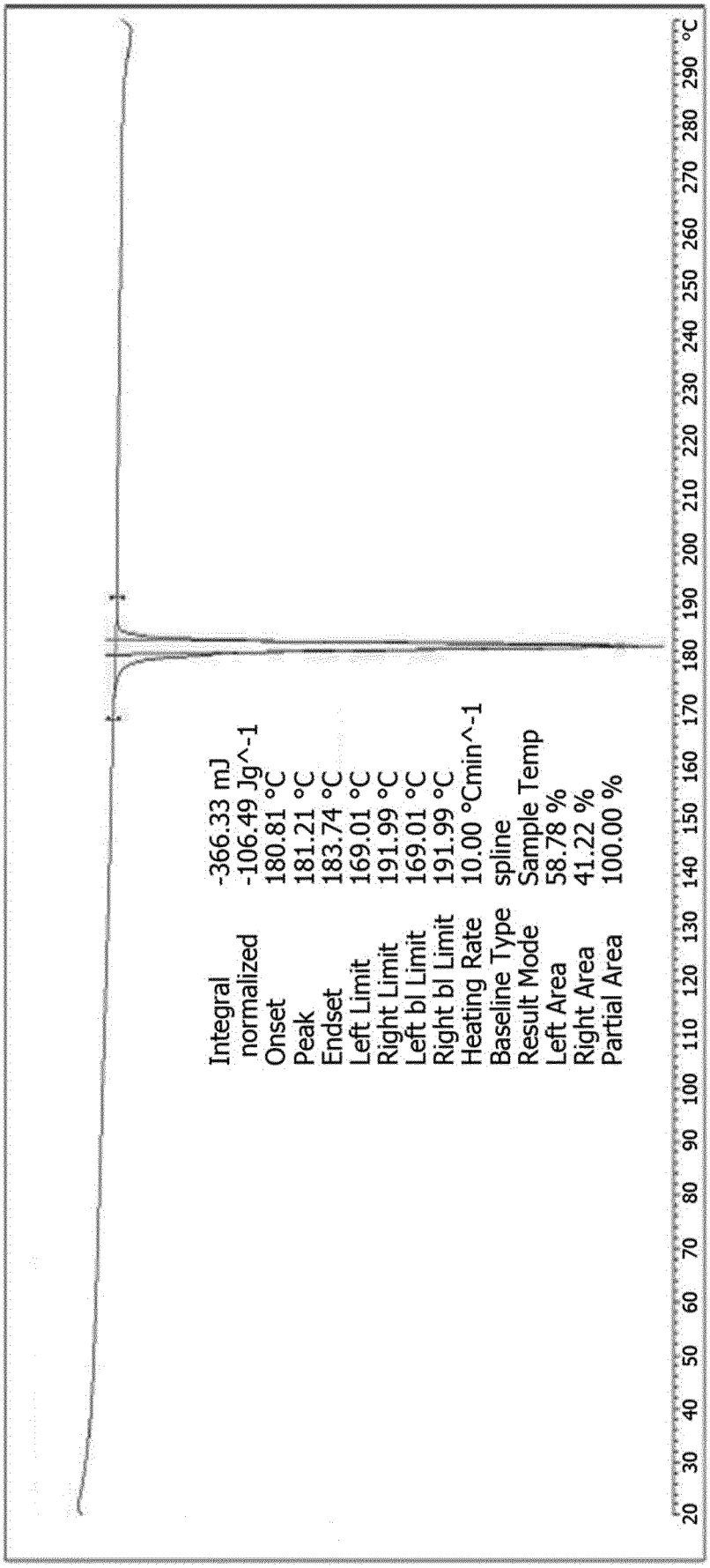
Integral -366.33 mJ
normalized -106.49 Jg^-1
Onset 180.81 °C
Peak 181.21 °C
Endset 183.74 °C
Left Limit 169.01 °C
Right Limit 191.99 °C
Left bl Limit 169.01 °C
Right bl Limit 191.99 °C
Heating Rate 10.00 °Cmin^-1
Baseline Type spline
Result Mode Sample Temp
Left Area 58.78 %
Right Area 41.22 %
Partial Area 100.00 %
20 30 40 50 60 70 80 90 100 110 120 130 140 150 160 170 180 190 200 210 220 230 240 250 260 270 280 290 °C

Fig.7

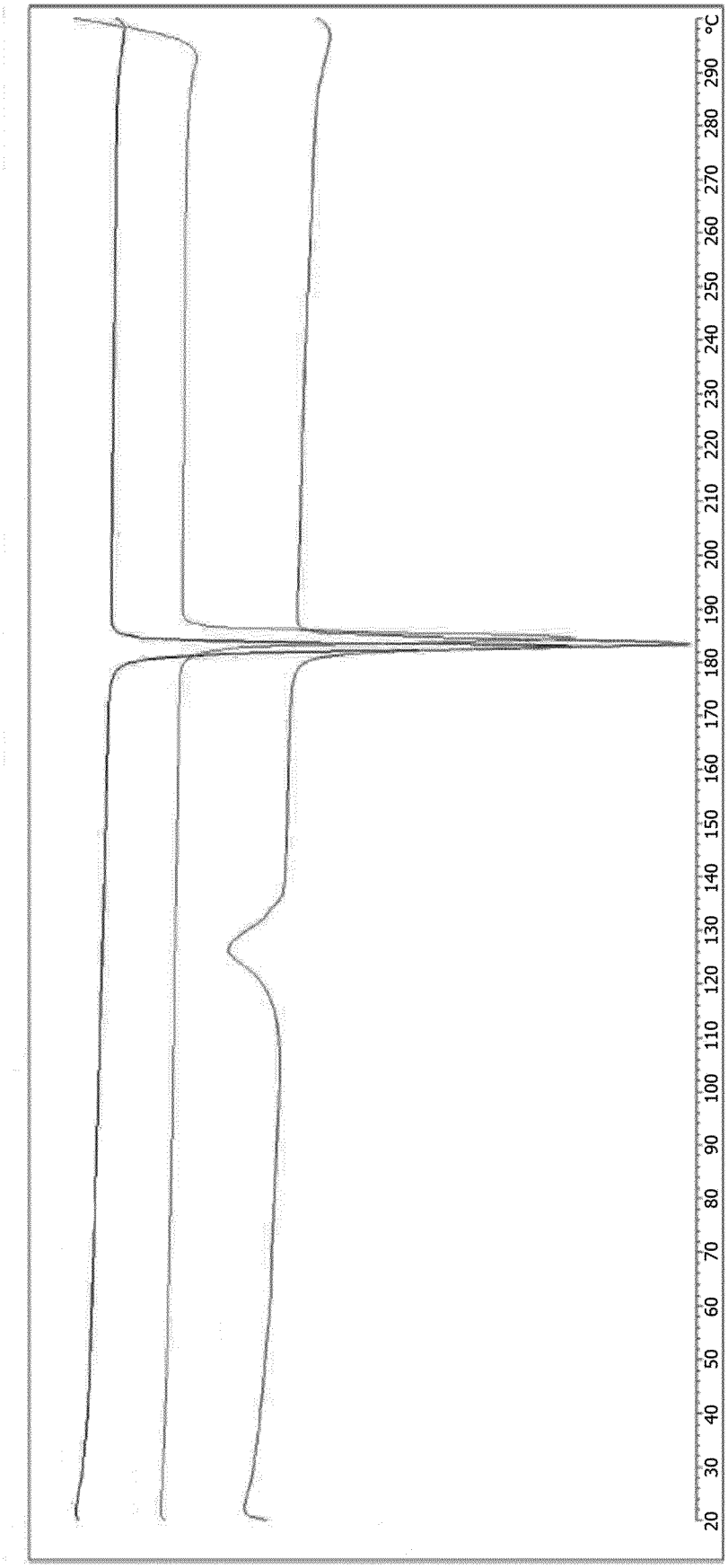
°C
290
280
270
260
250
240
230
220
210
200
190
180
170
160
150
140
130
120
110
100
90
80
70
60
50
40
30
20

Fig.8

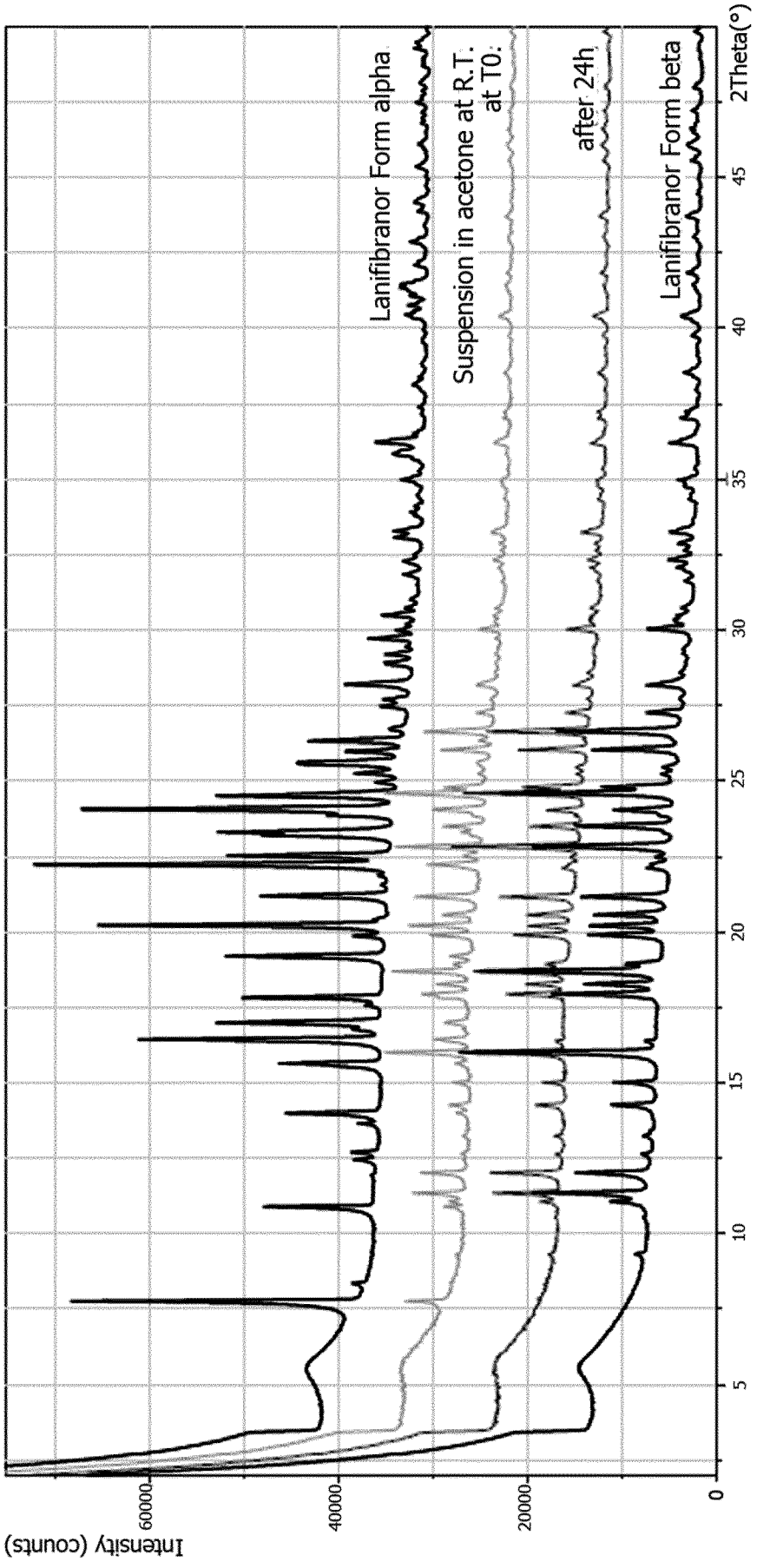
Lanifibranor Form alpha
Suspension in acetone at R.T.
at T0.
after 24h
Lanifibranor Form beta
2Theta(°)
Intensity (counts)
60000
40000
20000
0
5
10
15
20
25
30
35
40
45

Fig.9

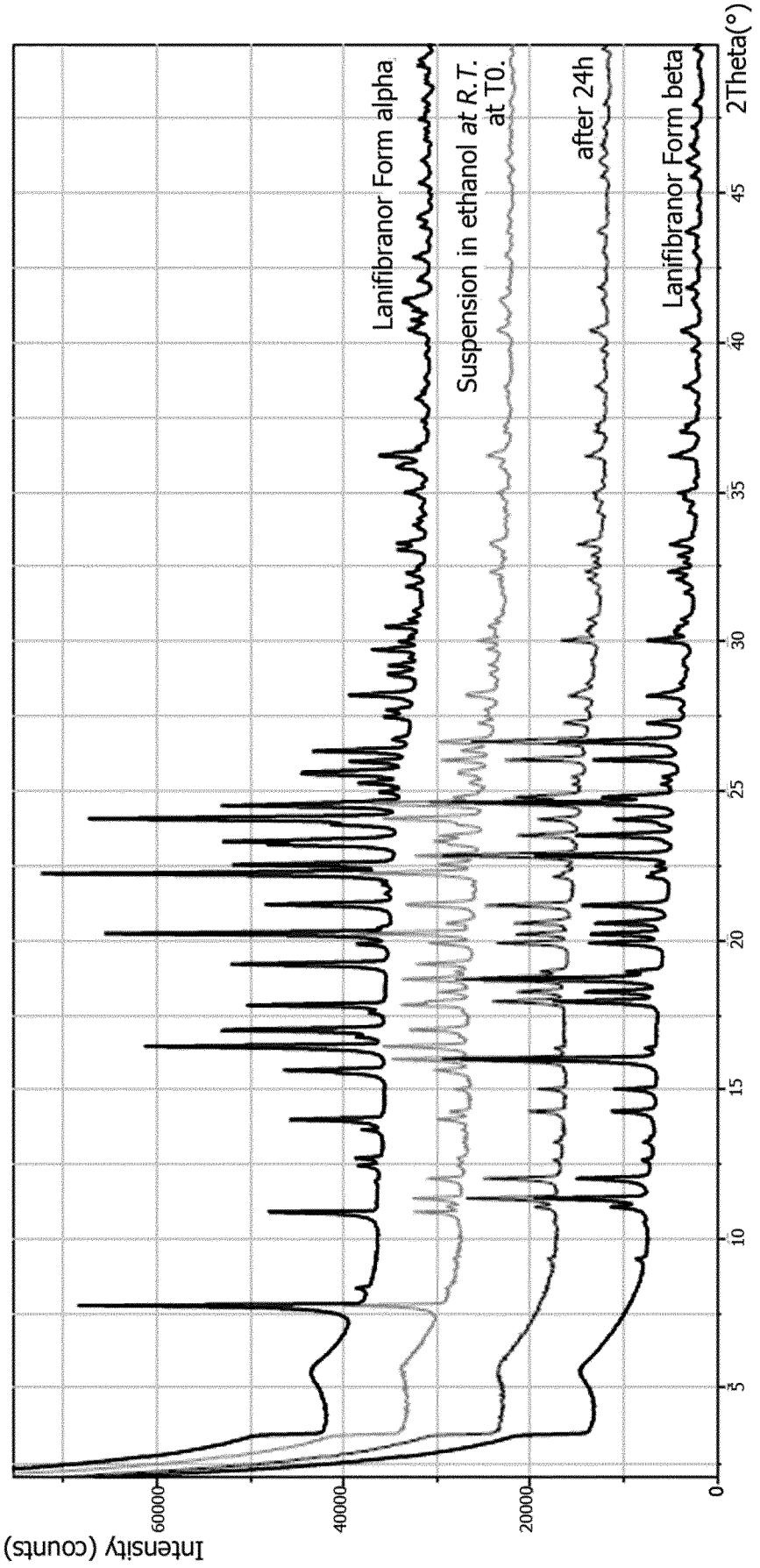
Lanifibranor Form alpha
Suspension in ethanol at R.T. at T0.
after 24h
Lanifibranor Form beta
2Theta(°)
Intensity (counts)
60000
40000
20000
0
5
10
15
20
25
30
35
40
45

Figure 10

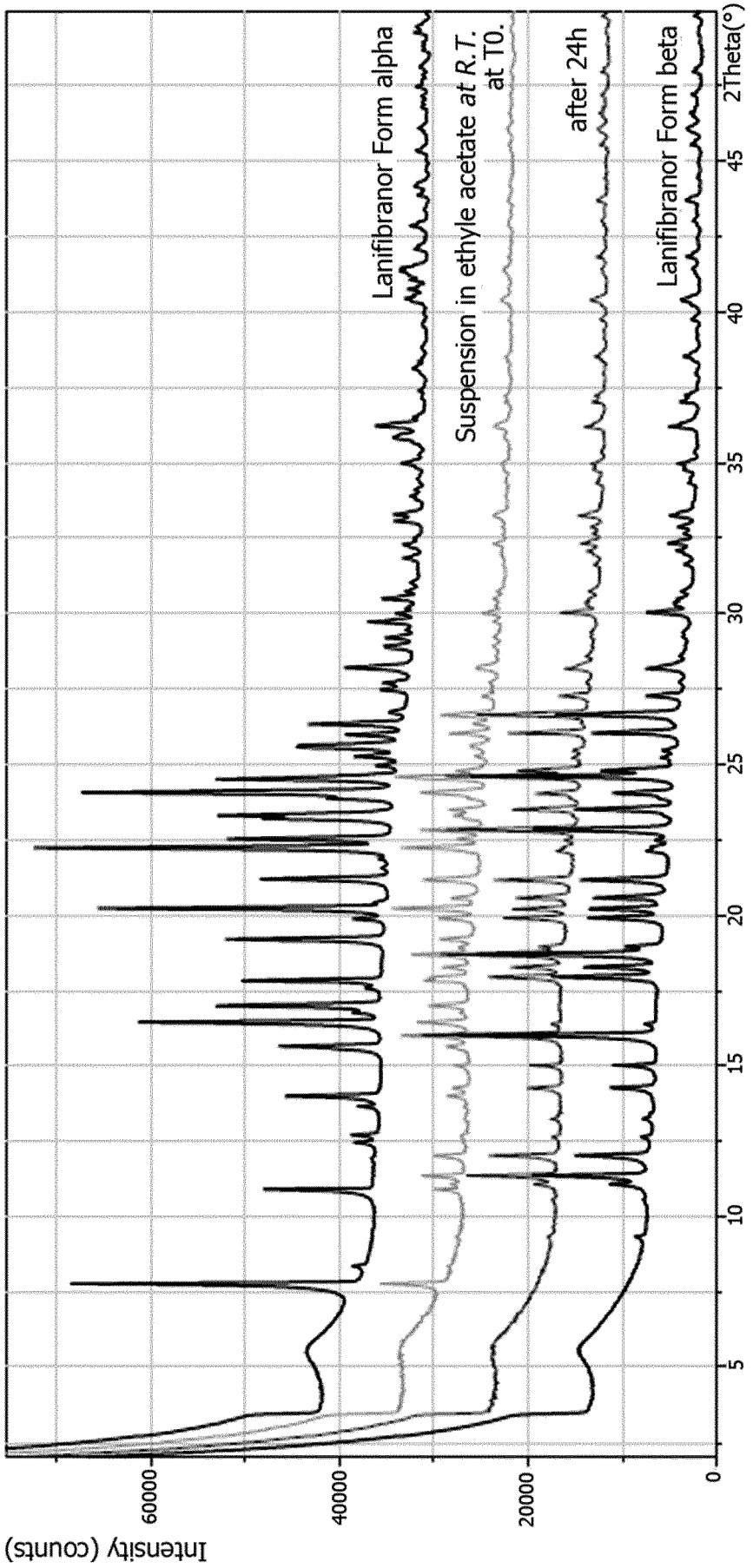
Lanifibranor Form alpha
Suspension in ethyle acetate at R.T.
at T0.
after 24h
Lanifibranor Form beta
2Theta(°)
Intensity (counts)
0
20000
40000
60000
5
10
15
20
25
30
35
40
45

Figure 11

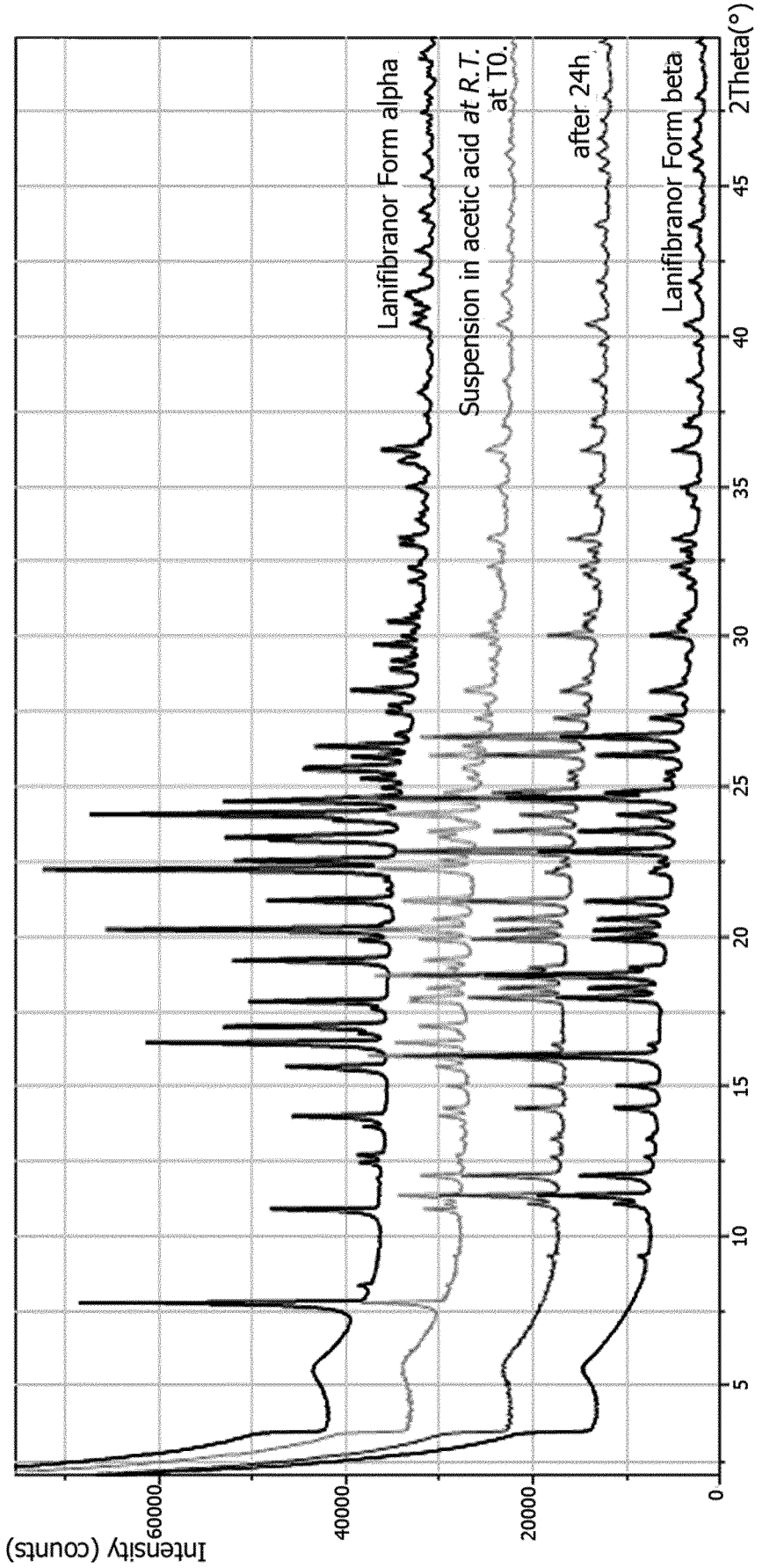
Lanifibranor Form alpha
Suspension in acetic acid at R.T.
at T0.
after 24h
Lanifibranor Form beta
2Theta(°)
Intensity (counts)
0
20000
40000
60000
5
10
15
20
25
30
35
40
45

Fig.12

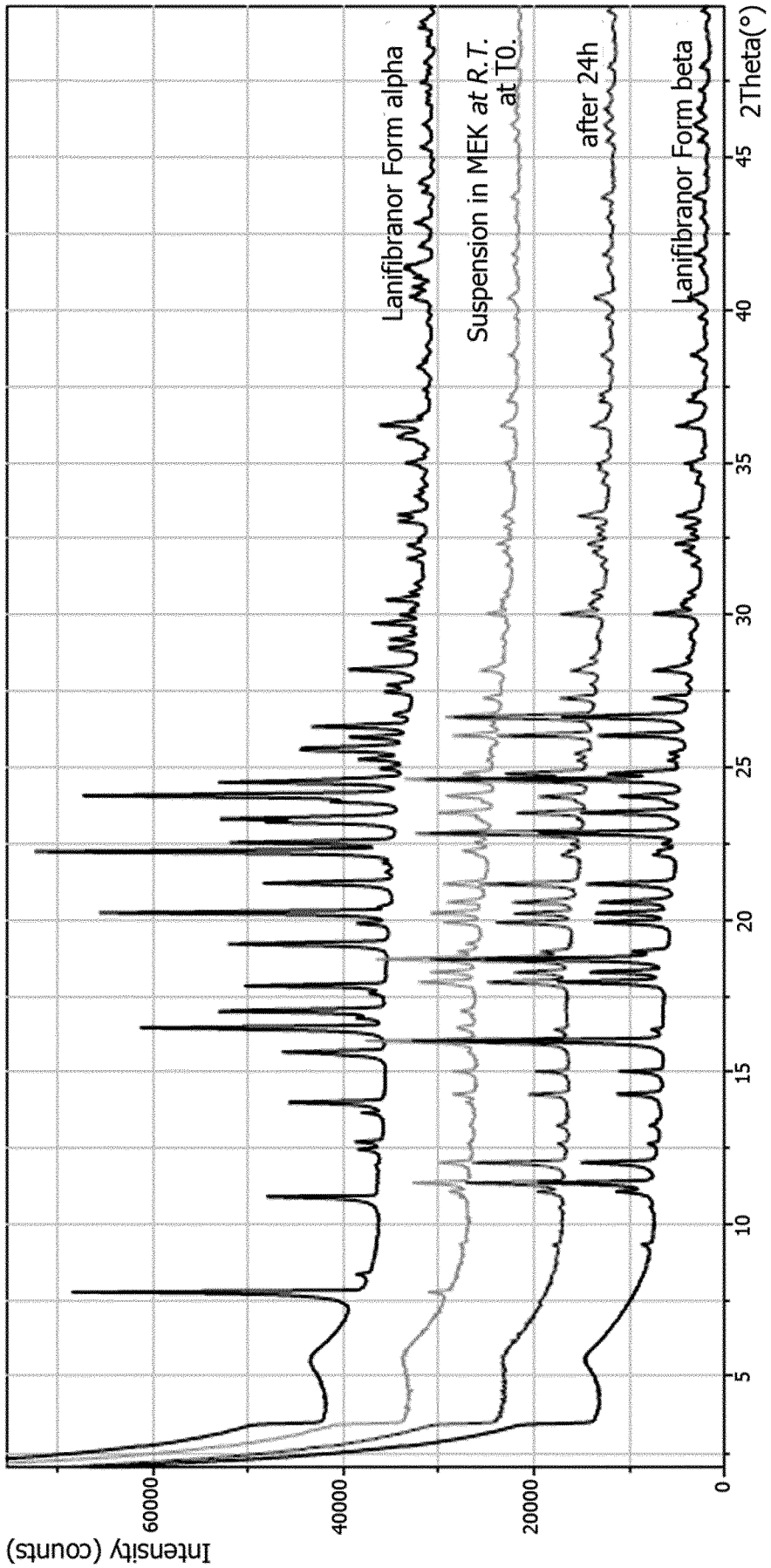
Lanifibranor Form alpha
Suspension in MEK at R.T.
at T0.
after 24h
Lanifibranor Form beta
2Theta(°)
Intensity (counts)
0
20000
40000
60000
5
10
15
20
25
30
35
40
45

Fig.13

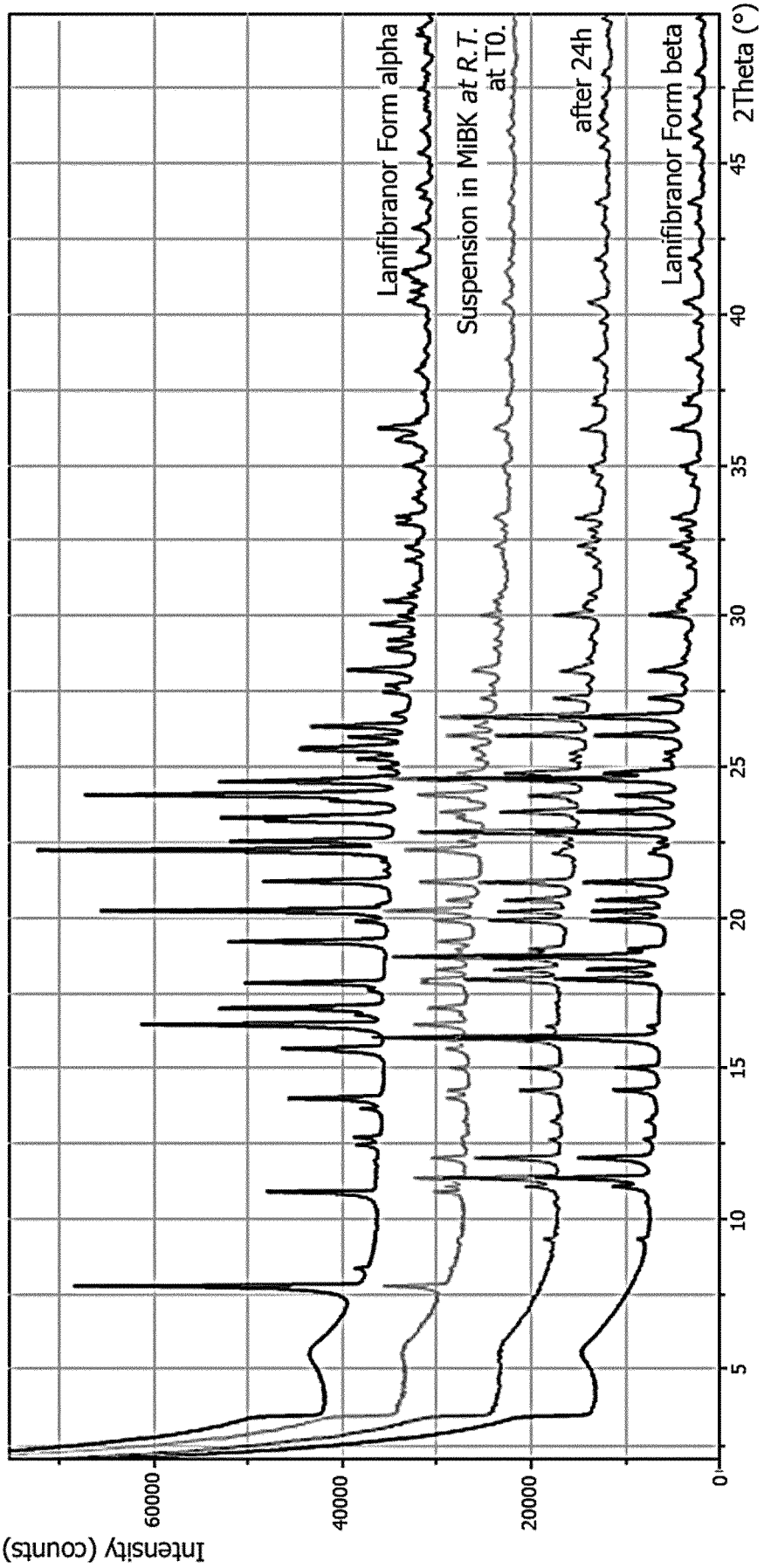
Lanifibranor Form alpha
Suspension in MiBK at R.T.
at T0.
after 24h
Lanifibranor Form beta
2Theta (°)
Intensity (counts)
0
20000
40000
60000
5
10
15
20
25
30
35
40
45

Fig.14

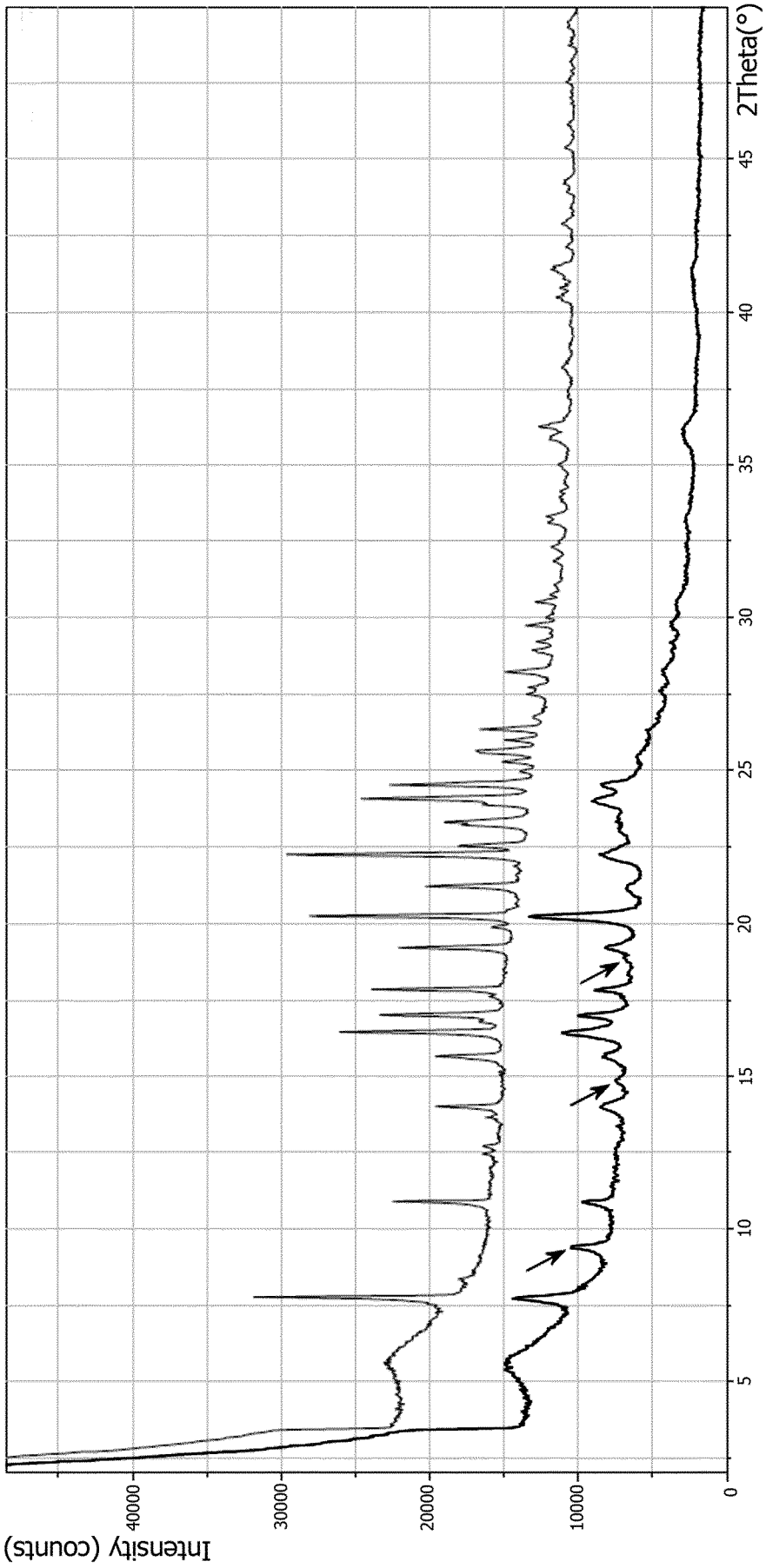
Intensity (counts)
40000
30000
20000
10000
0
5
10
15
20
25
30
35
40
45
2Theta(°)

Fig.15

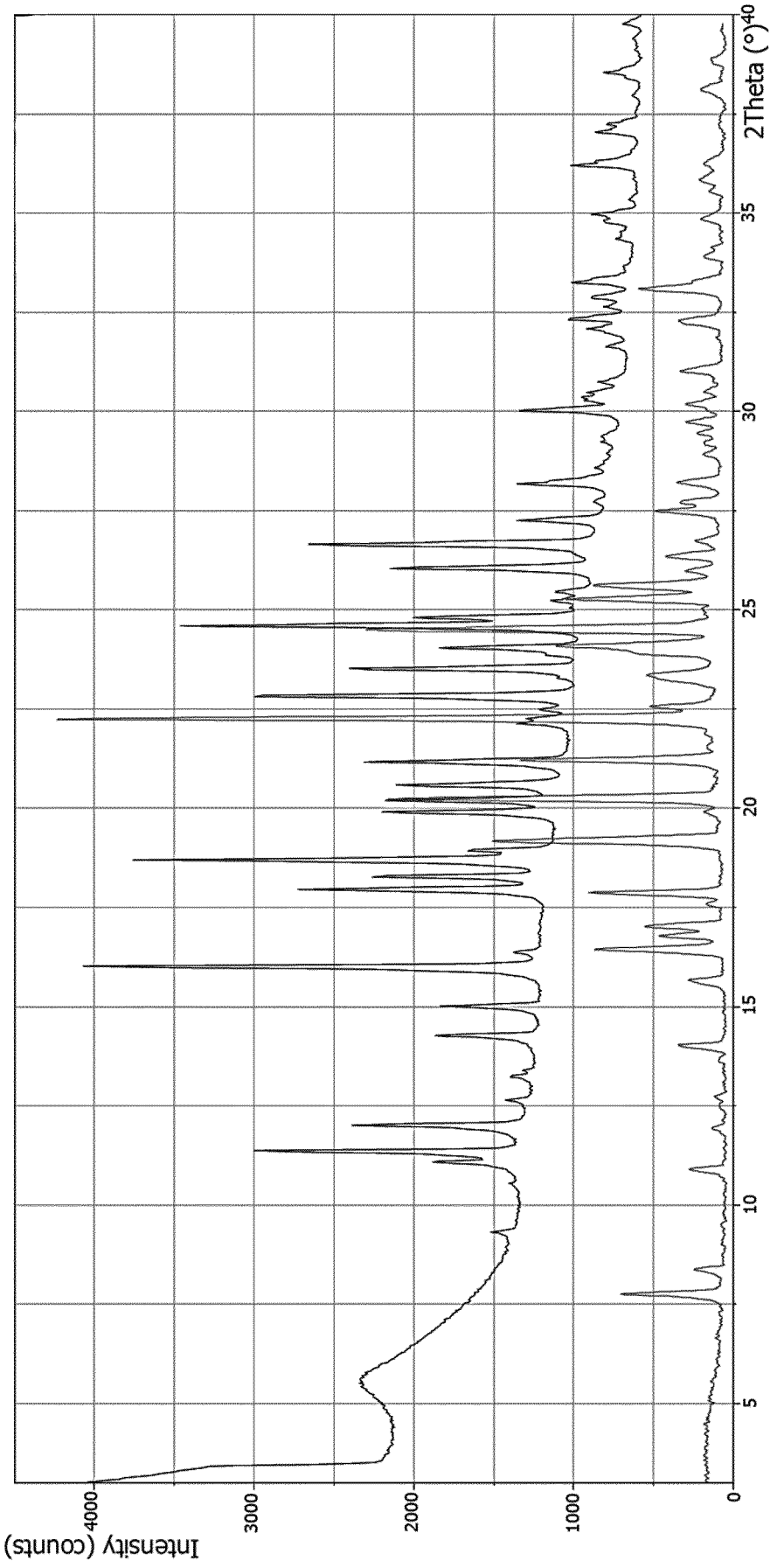
Intensity (counts)
4000
3000
2000
1000
0
5
10
15
20
25
30
35
40
2Theta (°)

Fig.16

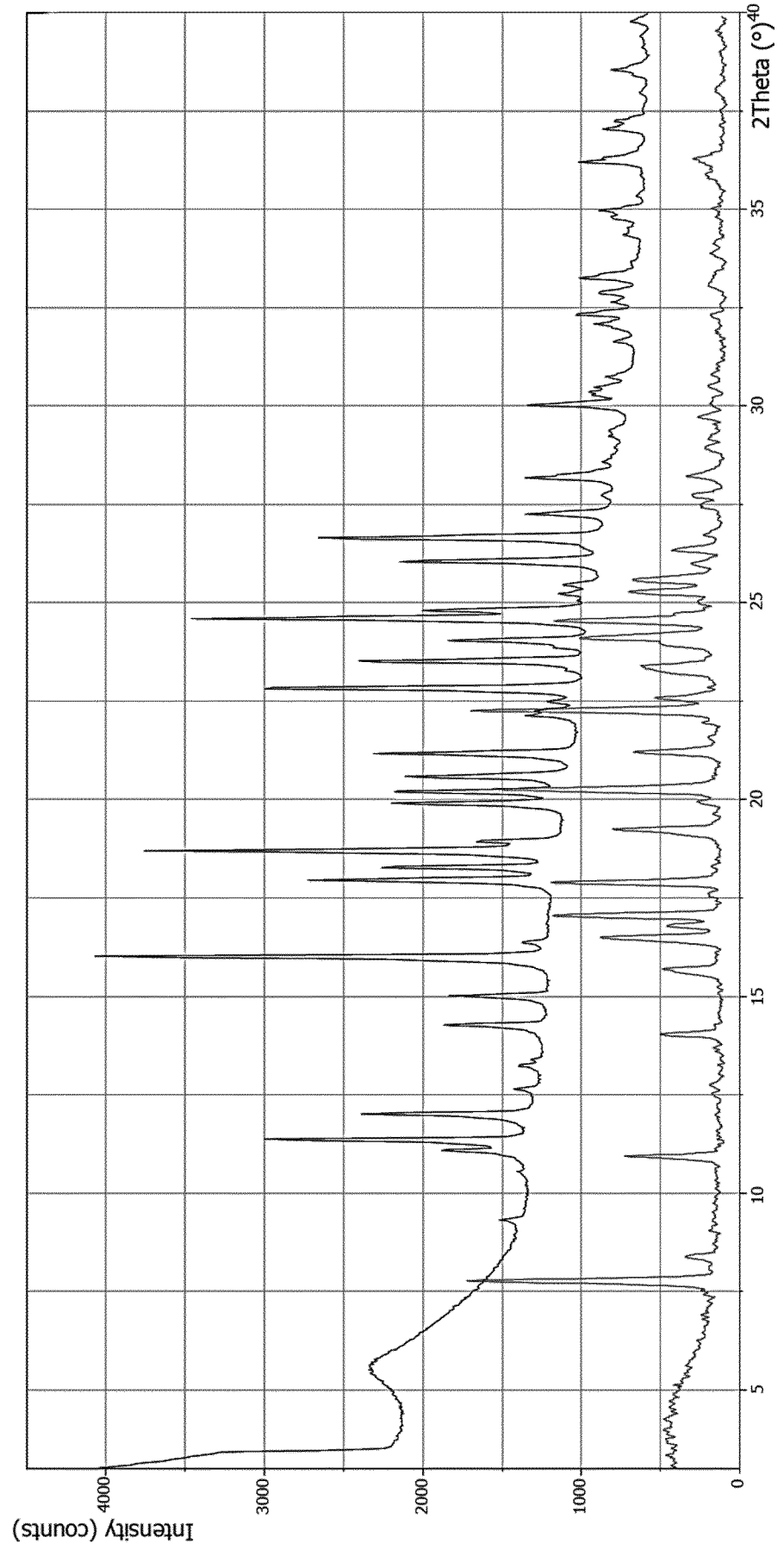
Intensity (counts)
4000
3000
2000
1000
0
5
10
15
20
25
30
35
40
2Theta (°)

Fig.17

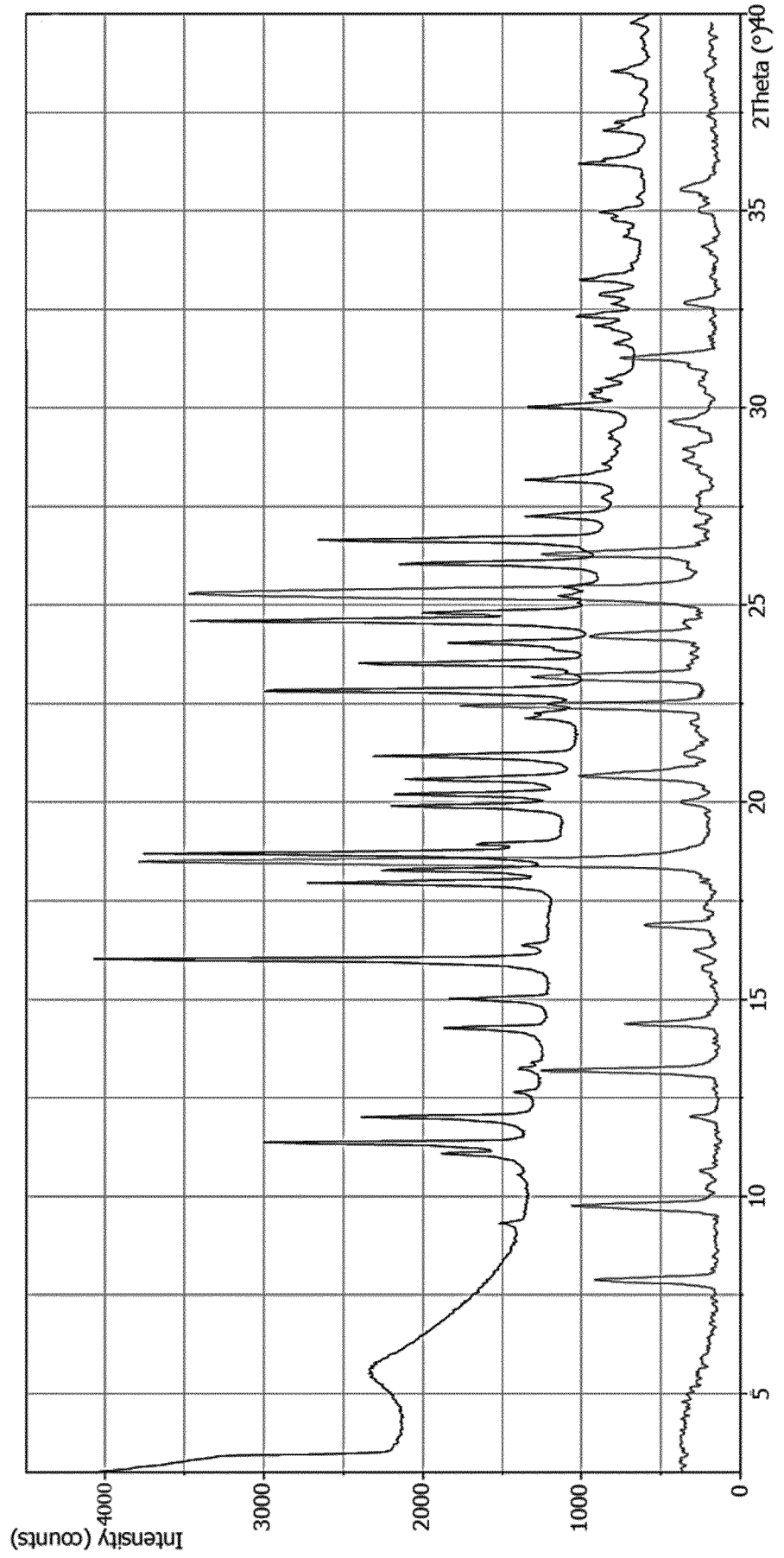
Intensity (counts)
4000
3000
2000
1000
0
5
10
15
20
25
30
35
40
2Theta (°)

Fig.18

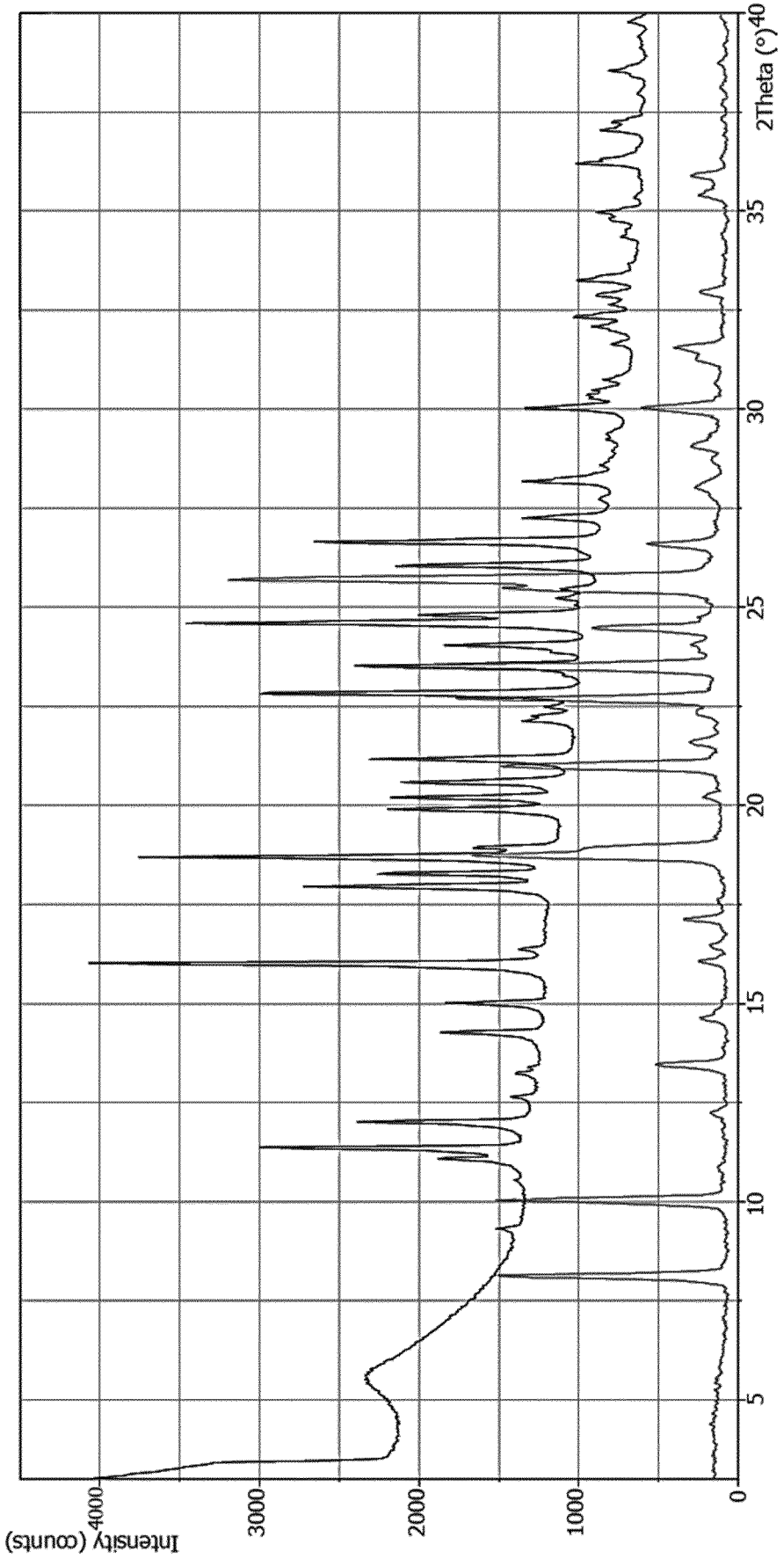
Intensity (counts)
4000
3000
2000
1000
0
5
10
15
20
25
30
35
40
2Theta (°)

Fig.19

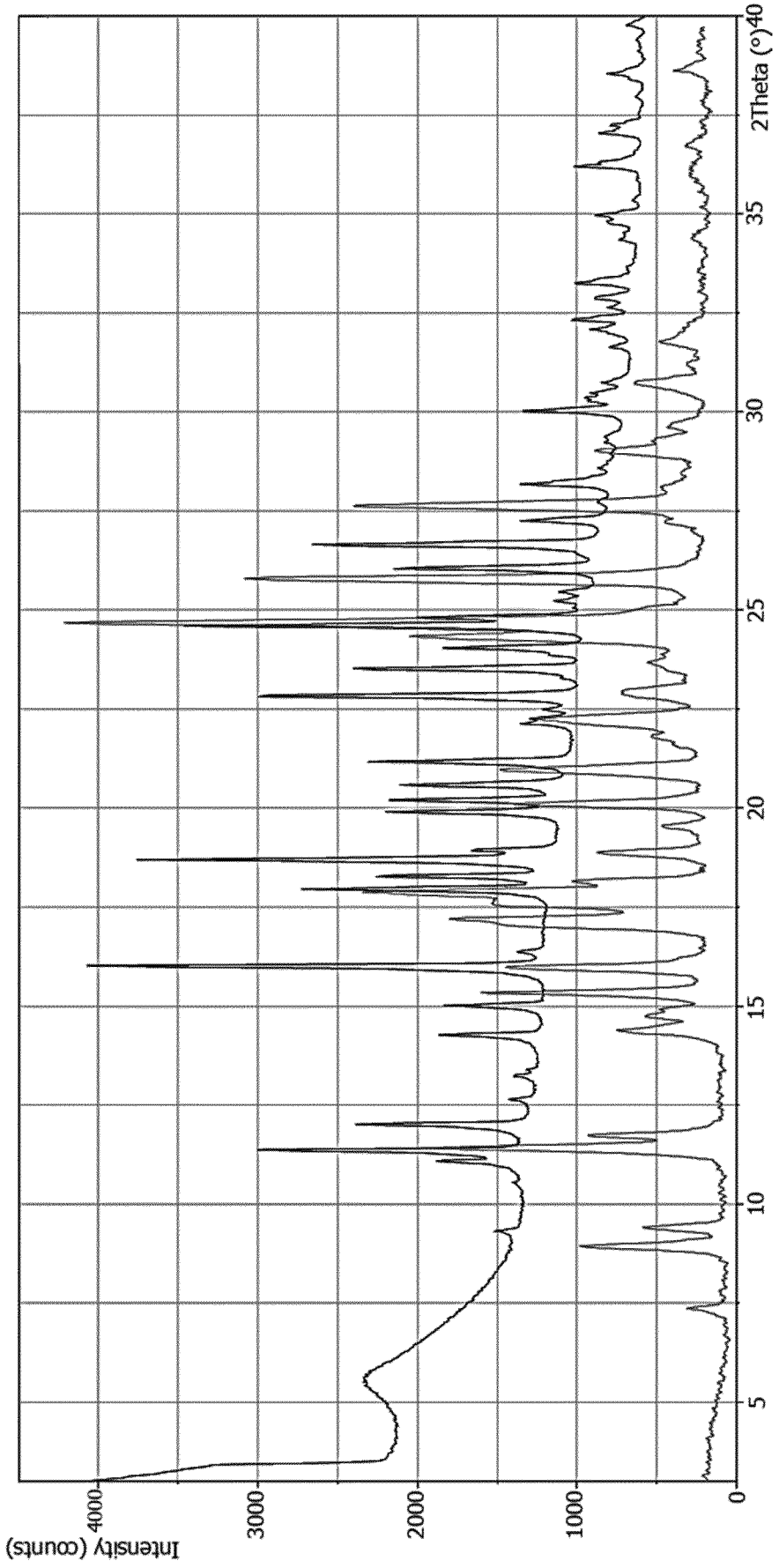
Intensity (counts)
0
1000
2000
3000
4000
5
10
15
20
25
30
35
40
2Theta (°)

Fig.20

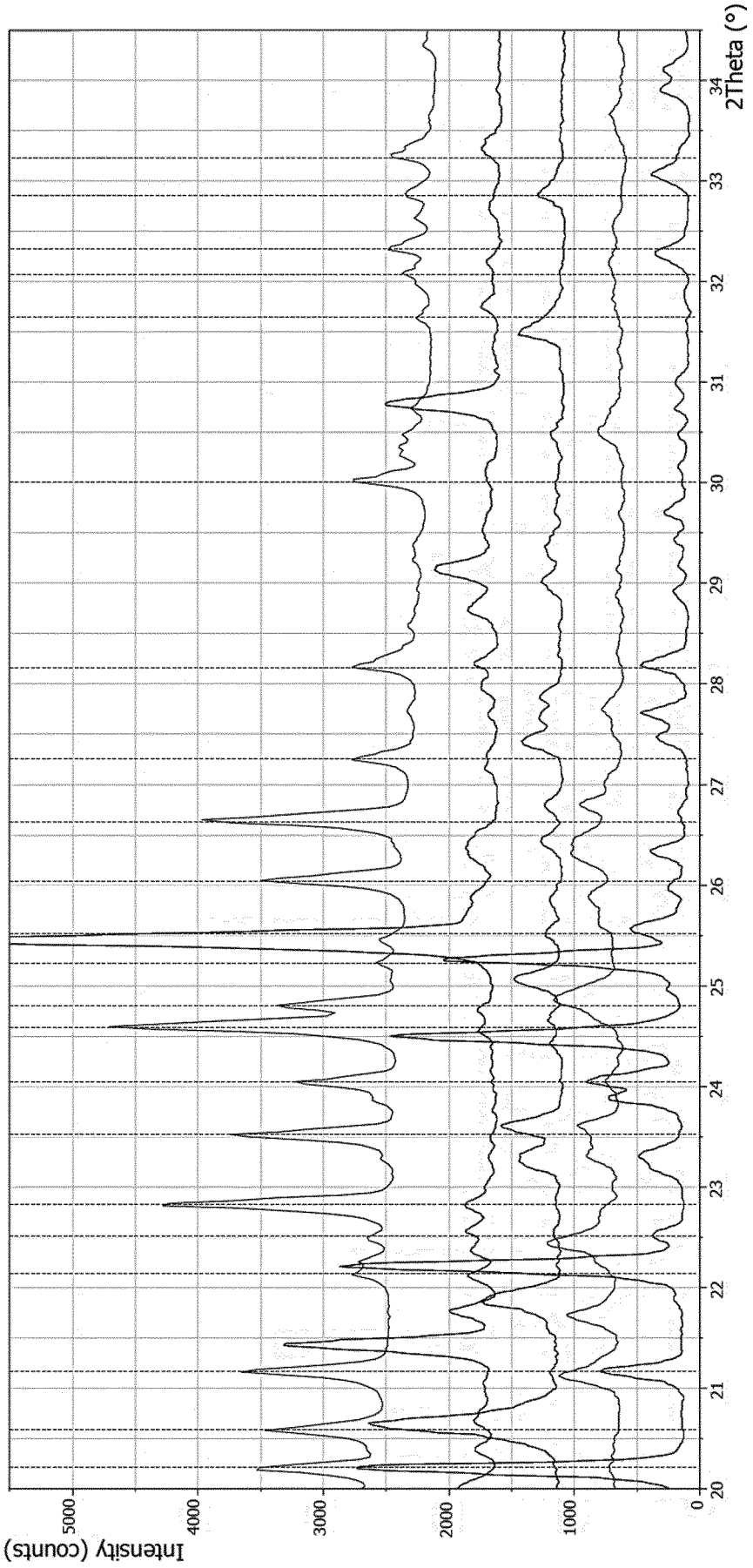
2Theta (°)
20
21
22
23
24
25
26
27
28
29
30
31
32
33
34
Intensity (counts)
0
1000
2000
3000
4000
5000

Fig.21

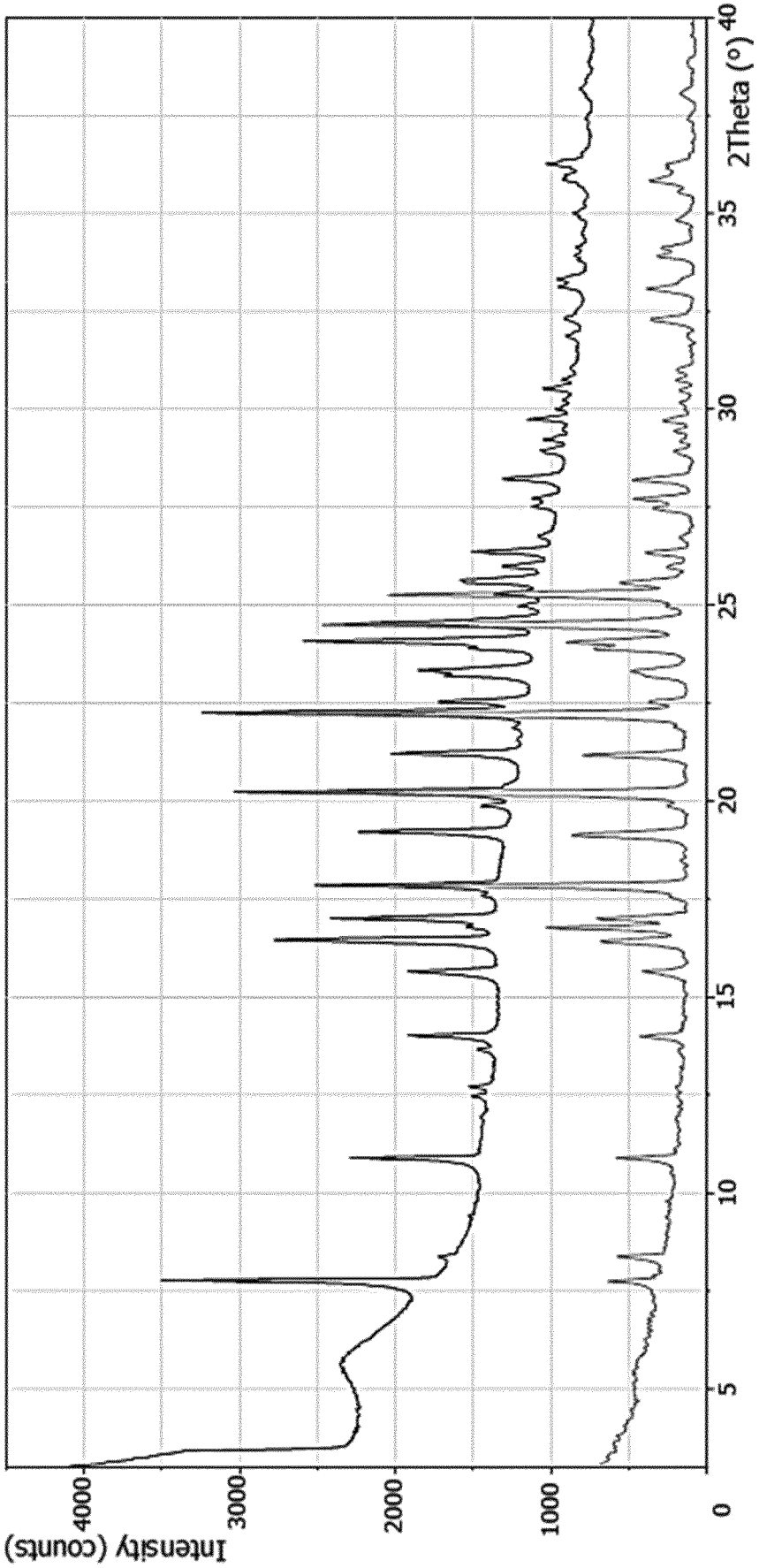
Intensity (counts)
4000
3000
2000
1000
0
5
10
15
20
25
30
35
40
2Theta (°)

Fig.22

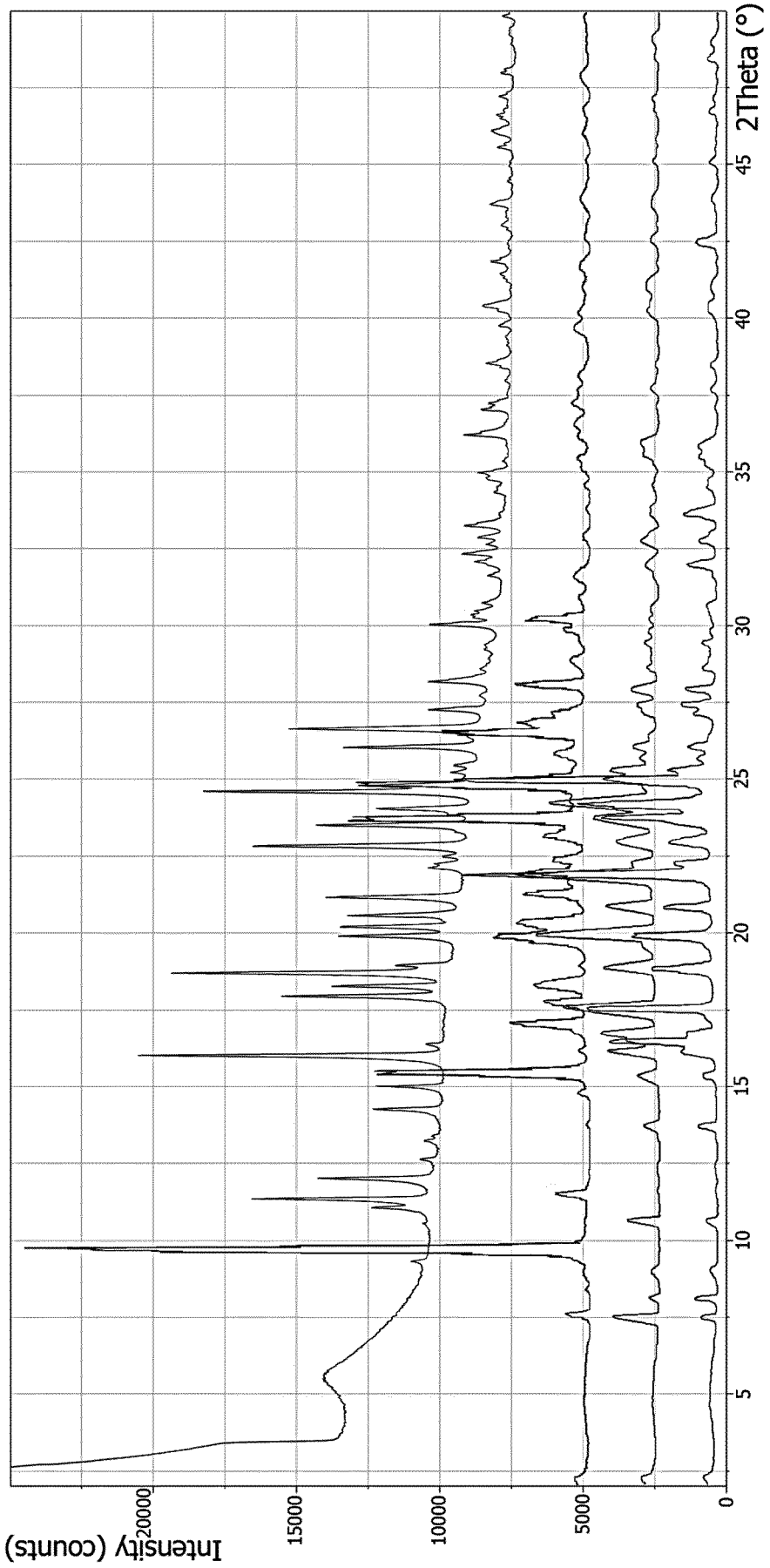
Intensity (counts)
20000
15000
10000
5000
0
5
10
15
20
25
30
35
40
45
2Theta (°)

Fig.23

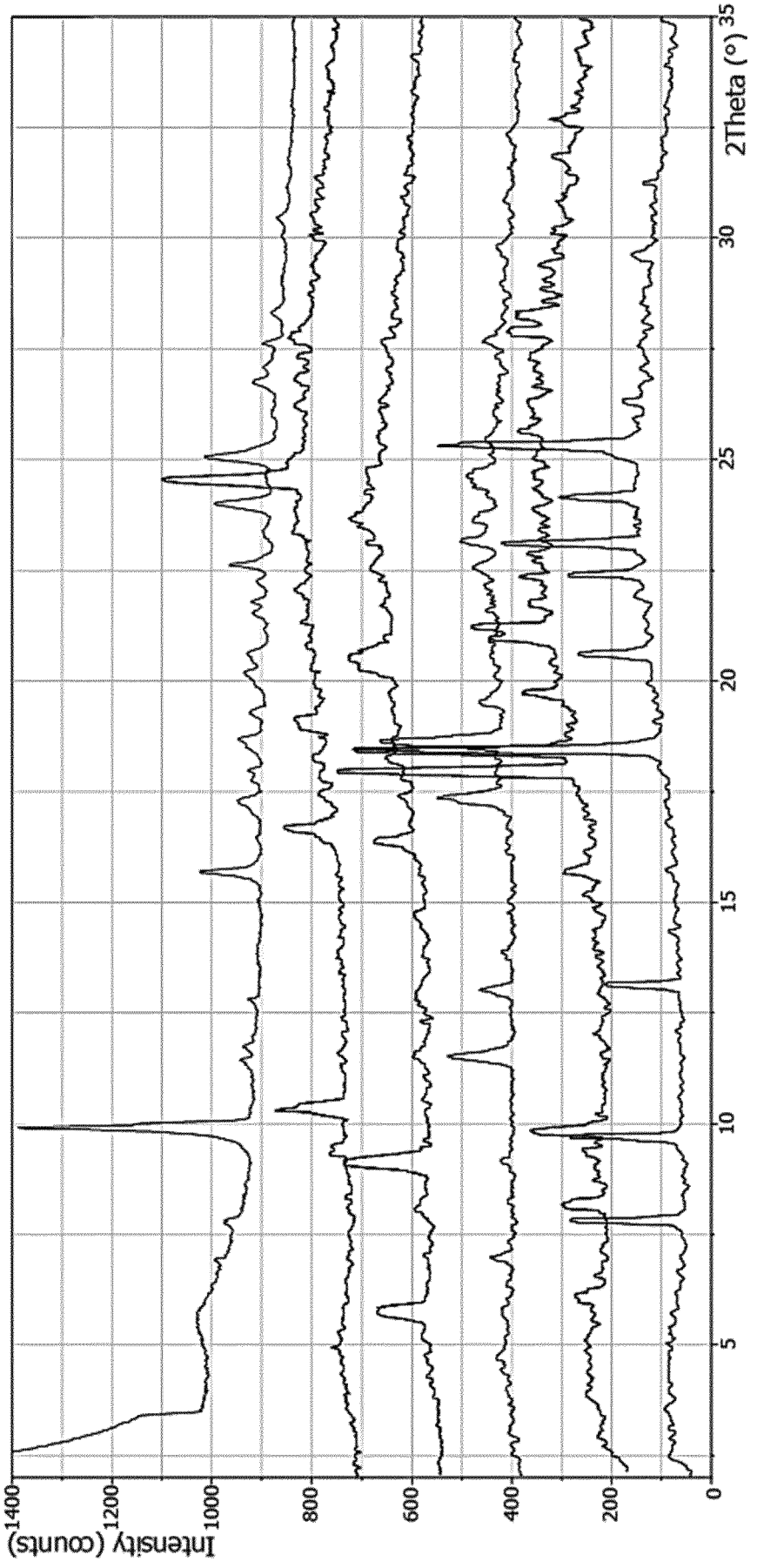
Intensity (counts)
1400
1200
1000
800
600
400
200
0
5
10
15
20
25
30
35
2Theta (°)

Fig.24

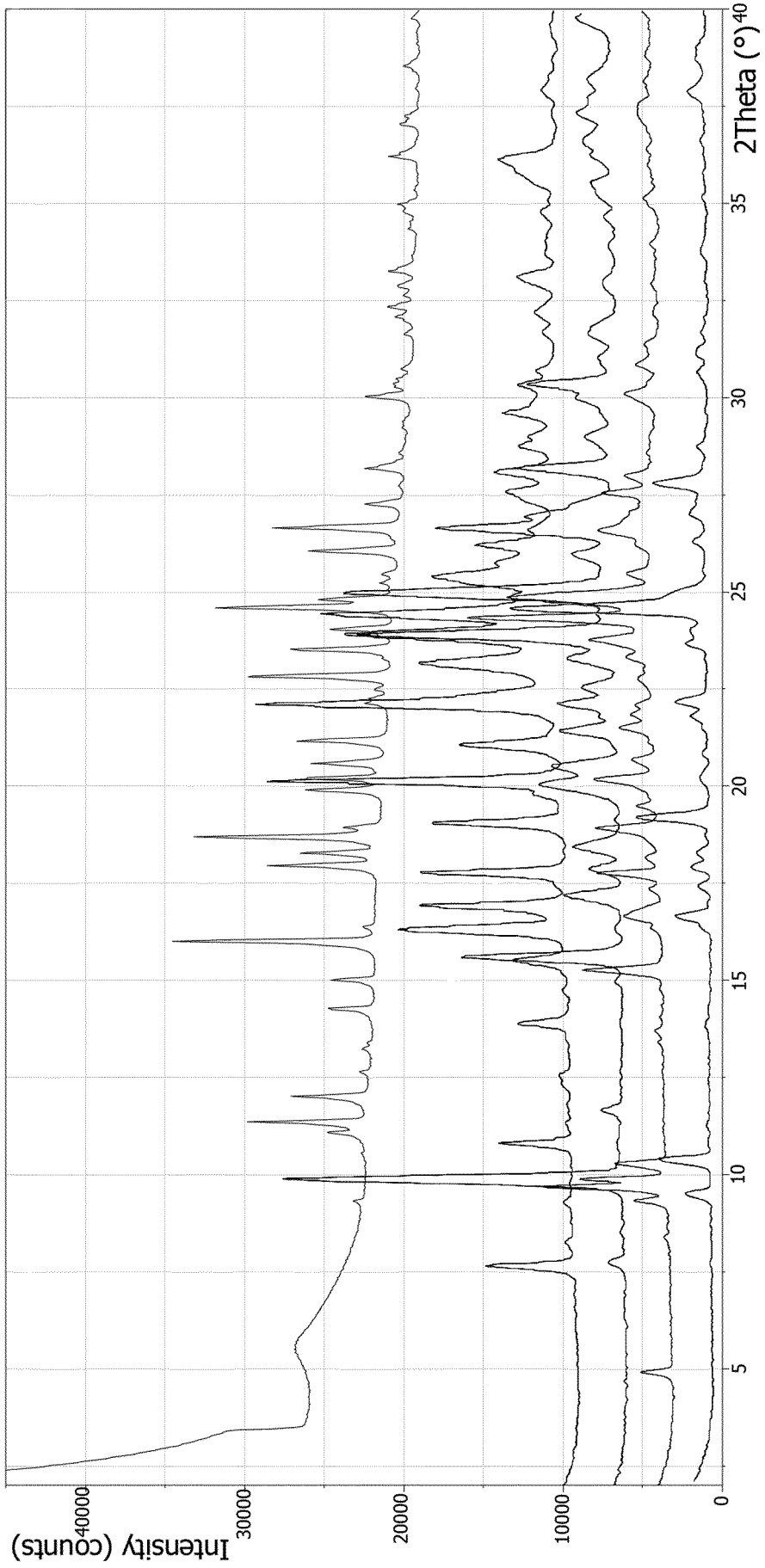
Intensity (counts)
40000
30000
20000
10000
0
5
10
15
20
25
30
35
40
2Theta (°)

Fig.25

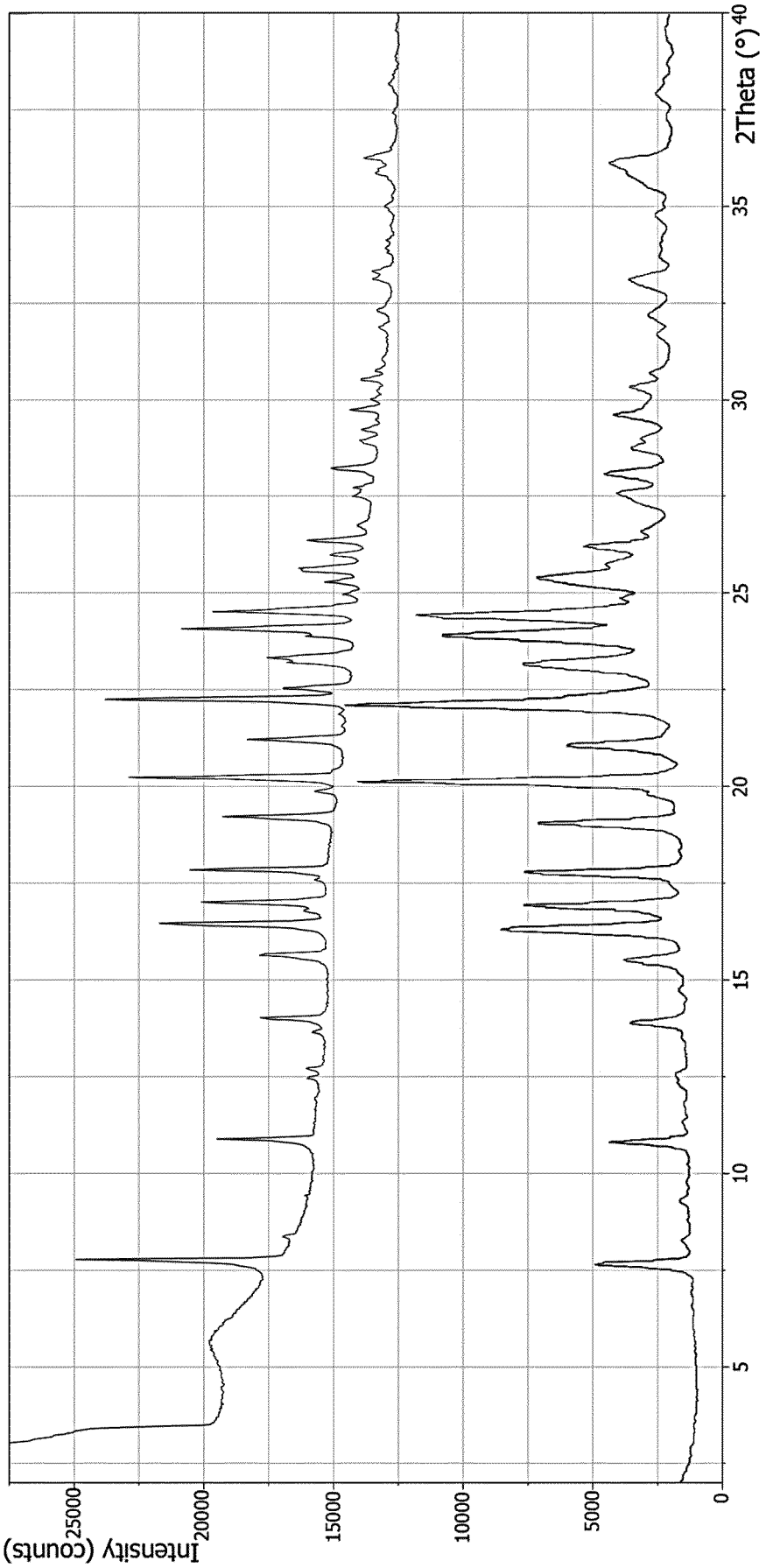
Intensity (counts)
25000
20000
15000
10000
5000
0
5
10
15
20
25
30
35
40
2Theta (°)

Fig.26

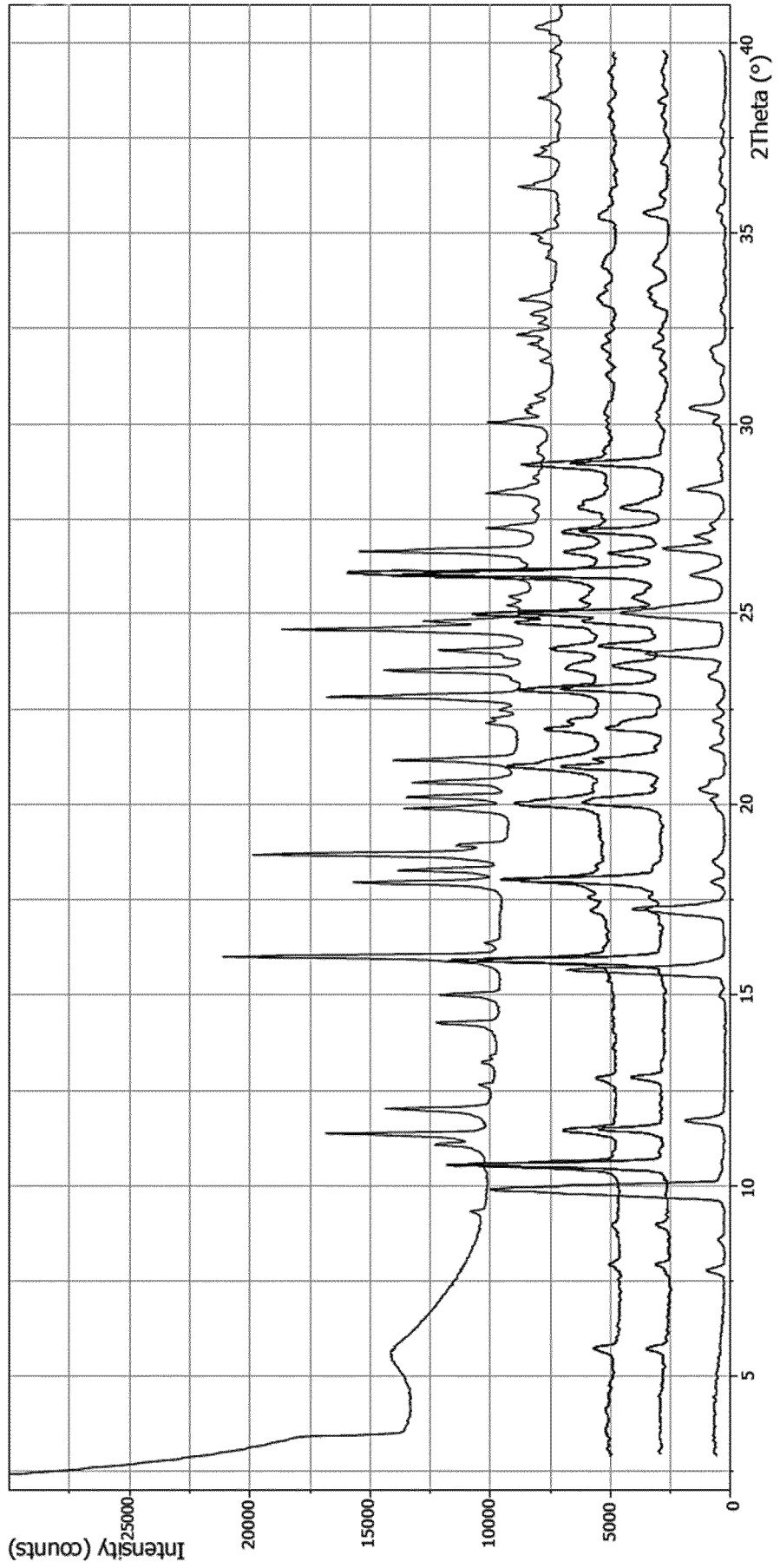
Intensity (counts)
25000
20000
15000
10000
5000
0
5
10
15
20
25
30
35
40
2Theta (°)

Fig.27